

Intestinal B cells license metabolic T-cell activation and contribute to fibrosis via IgA-FcR signalling in NASH

Elena Kotsiliti, Valentina Leone, Svenja Schuehle, Olivier Govaere, Hai Li, Monika J. Wolf, Helena Horvatic, Sandra Bierwirth, Jana Hundertmark, Donato Inverso, Laimdota Zizmare, Avital Sarusi-Portuguez, Revant Gupta, Tracy O'Connor, Anastasios D. Giannou, Ahmad Mustafa Shiri, Yehuda Schlesinger, Maria Garcia Beccaria, Charlotte Rennert, Dominik Pfister, Rupert Öllinger, Iana Gadjalova, Pierluigi Ramadori, Mohammad Rahbari, Nuh Rahbari, Marc Healy, Mirian Fernández-Vaquero, Neda Yahoo, Jakob Janzen, Indrabahadur Singh, Chaofan Fan, Xinyuan Liu, Monika Rau, Martin Feuchtenberger, Eva Schwaneck, Sebastian J Wallace, Simon Cockell, John Wilson-Kanamori, Prakash Ramachandran, Celia Kho, Timothy J Kendall, Anne-Laure Leblond, Selina J. Keppler, Piotr Bielecki, Katja Steiger, Maike Hofmann, Karsten Rippe, Horst Zitzlesberger, Achim Weber, Nisar Malek, Tom Lüdde, Mihael Vucur, Hellmut G. Augustin, Richard Flavell, Oren Parnas, Roland Rad, Olivier Pabst, Neil C. Henderson, Samuel Huber, Andrew Macpherson, Percy Knolle, Manfred Claasen, Andreas Geier, Christoph Trautwein, Kristian Unger, Eran Elinav, Ari Waisman, Zeinab Abdullah, Dirk Haller, Frank Tacke, Quentin M. Anstee, Mathias Heikenwalder

Table of contents	
Supplementary materials and methods.....	2
Supplementary tables.....	22
Supplementary references.....	27
Supplementary figure legends.....	30
Supplementary figures.....	39

Supplementary materials and methods

Mice, diets and treatments

4-week-old male C57BL/6J mice were purchased from Charles River, and all strains of genetically-altered mice were on a C57BL/6J background. Control mice were matched by genetic background, age and sex. Mice were housed at the German Cancer Research Center (DKFZ) and at the University Hospital Zurich (Labortierkunde/LTK)). Animals were maintained under specific pathogen-free conditions, and experiments were performed in accordance with German and Switzerland Law and registered at the Landesamt für Natur, Umwelt und Verbraucherschutz Nordrhein-Westfalen (LANUV) (approval no. G11/16, G7/17, AZ 84-02.04.2017.A061). *JH^{-/-}* and *μMT* mice were under the license numbers ZH136/2014 and ZH217/2012. *IgMi* mice were thankfully provided by Prof. Dr. A. Waisman (animal permission: 23 177-07/G12-1-057). 4-weeks old male C57Bl/6N germ-free mice were provided by Prof. Dr. Dirk Haller, and the diet experiments took place in his germ-free facility at the Technical University of Munich (TUM) (School of Life Sciences Weihenstephan) according to the German Law (Regierung von Oberbayern, approval no. 55.2-1-54-2532-72-2015). Kaede transgenic mice¹ were provided by Prof. Dr. Samuel Huber and the diet experiments took place at the University Medical Center Hamburg-Eppendorf in accordance with the institutional review board Behörde für Justiz und Verbraucherschutz, Lebensmittelsicherheit und Veterinärwesen (approval no. G13/17). 4-week-old male mice were fed ad libitum: normal diet (ND) (Provimi Kliba, Switzerland), choline-deficient high-fat diet (CD-HFD) (Research Diets; D05010402), western diet (Ssniff Spezialdiäten GmbH, E15723-34),

CDA-HFD (Ssniff Spezialdiäten GmbH, E15673-940), and western diet with trans-fats (WD-HTF) (Research Diets; D16022301). Animals used for *ex vivo* experiments were treated in accordance with the “German Animal Protection Law” and the guidelines of the animal care unit at our university (Haus für experimentelle Therapie, Bonn, Germany) and approved by the relevant North Rhine-Westphalian state agency for Nature, Environment and Consumer Protection (LANUV, Germany) under the file reference LANUV84-02.04.2014.A137. At the end of the experiments, animals were sacrificed, and the liver, spleen, small intestine and serum were harvested for analysis.

B cells depletion experiments

B cell depletion was carried out using the CD20 antibody against mouse from Genentech (clone 5D2). 4 weeks old mice were put on CD-HFD for 4 months, followed by anti-CD20 treatment with intraperitoneal (i.p.) injections of 200µg, once per week, with pause one week in between, for a total duration of treatment of 6 weeks.

Kaede mice

For photoconversion, the small intestine of anaesthetized Kaede transgenic mice, which constitutively express a photoconvertible fluorescent protein in all cells, was subjected to lighting using a Blue Wave LED Prime UVA (Dymax), essentially as described before². At 6 months, upon different diet feeding (ND, WD-HTF or CD-HFD), the small intestine of Kaede mice was photo-converted to label cells from green to red, enabling direct tracing of cells from the small intestine to other tissues. The mice were sacrificed 48h after photoconversion and Flow cytometry of livers was performed.

Confocal microscopy for Kaede mice

Liver samples derived from Kaede transgenic mice were observed with a confocal microscope (Leica, SP5) and illuminated with a laser with 488 nm for green Kaede and 561 nm for photoconverted Kaede, respectively; these emission signals were obtained by setting the wavelength range at 500–550 nm and 570–620 nm, respectively.

Measurement of liver triglycerides

Liver triglycerides were measured by crushing 20 - 50 mg of tissue in liquid with a pestle and adding 250µl 0.9% NaCl. After incubation on heat block for 10min, RT, 450rpm, 250µl ethanolic 0.5M KOH was added, samples were vortexed and incubated for 30min, 71°C, 450rpm. 500µl 0.15M MgSO₄ was added, and samples were vortexed. After centrifugation for 10min, RT, 13,000g supernatants were collected and analyzed by using optical densitometry O.D. 505 with 1:4 diluted liver samples by GPO-PAP from Roche Diagnostics³.

Intraperitoneal glucose tolerance test

After overnight fasting, mice were i.p injected with 5µl/gr body weight of a 20% glucose solution, blood glucose was measured using Accu-chek Performa Glucometer at the indicated time intervals (15, 30, 60 and 120 minutes post glucose administration), by puncturing the lateral tail vein³.

Measurement of serum parameters

Serum was isolated from the heart blood after sacrifice, and parameters were measured by using either a Fuji DRI-CHEM NX500i machine with a commercially available test application from FUJIFILM for ALT, cholesterol and triglycerides or analyzing parameters on a Cobas Reader in collaboration with the Institute for Clinical Chemistry and Pathobiochemistry, Technical University of Munich³.

CCl₄ injection

For the acute liver injury experiment, liver mice received one intraperitoneal application of Carbon tetrachloride (CCl₄) (Merck, Darmstadt, Germany) dissolved in corn oil at a concentration of 0.6 mL/kg body weight. Mice were sacrificed after 36 hours from the injection. For long-term injections, CCl₄ was intraperitoneally injected at 0.6 mL/kg body weight (BW) twice per week for 8 weeks.

RNA isolation from murine livers and quantitative real-time PCR

Total RNA was isolated from snap-frozen liver tissues according to the manufacturer's protocol using RNeasy Mini Kit (Qiagen). The quantity and quality of the RNA were determined spectroscopically using a Nanodrop analyzer (Thermo Scientific). 1 µg of purified RNA was subsequently transcribed into cDNA using Quantitect Reverse Transcription Kit (Qiagen) according to the manufacturer's protocol. Quantitative RT-PCR was performed using Fast Start SYBR Green Master Rox (Roche). Primers were designed using Primer-Blast. For mRNA expression analysis, quantitative real-time PCR was performed in duplicates in 384-well plates using Fast Start SYBR Green Master Rox (Roche) on a 7900 HT qRT-PCR system (Applied Biosystems, Life

Technologies Darmstadt, Germany). Relative mRNA levels were calculated according to the $\Delta\Delta C_t$ relative quantification method and were normalized to levels of a housekeeping gene (GAPDH). The data were normalized to the expression of the housekeeping gene and analyzed using GraphPad Prism software version 9.3 (GraphPad Software)³.

For a list of all used primers for RT-qPCRs, refer to **Table S1**.

Library preparation for bulk murine liver tissue RNA sequencing (RNA-Seq)

The libraries were prepared with 30 ng of total RNA using QuantSeq 3' mRNA-Seq Library Prep Kit FWD for Illumina (Cat.No. 015.96, Lexogen GmbH, Austria) with single-indexing, according to the manufacturer's instruction for low-quality RNA. To determine the optimal cycle number for the library amplification the PCR Add-on Kit from Illumina (Cat.No. 020.96, Lexogen GmbH, Austria) was used. The individual libraries were eventually amplified with 24 PCR cycles.

Flow cytometry and FACS: Isolation and staining of lymphocytes

Mice were sacrificed with CO₂, and livers, spleens, blood and small intestines were dissected. Livers were incubated for up to 35min at 37°C with digestion buffer (Collagen IV 1:10 (60 U f.c.) and DNase I 1:100 (25µg/ml f.c.)) and subsequently passed through a 100µm filter. Livers were washed with RPMI1640 (Cat.No.11875093) medium and subsequently centrifuged for 7min/300g/4°C. Lymphocyte enrichment was achieved by a 2-step Percoll gradient (20ml 25% Percoll/HBSS underlay with 20ml 50% Percoll/HBSS) and centrifugation for 15min/1800g/4°C (Acc:1 Dcc:0). Leukocytes were collected, washed with HBSS, centrifuged for 10min/700g/4°C, counted and transferred to a 15ml Falcon for a final washing step with FACS buffer (PBS

supplemented with v/v 0.4% 0.5M EDTA pH= 8 and w/v 0.5% albumin fraction V (Cat.No.90604-29-8)). Isolation of splenic lymphocytes was done by passing spleens through a 100µm mesh and subsequent washing. Isolation of blood-derived lymphocytes was done by collection of blood in FACS buffer and performing erythrocyte lysis two times using ACK-buffer 1x 2ml for 5 min RT and then washing. Afterwards, an erythrocyte lysis using ACK-buffer 1x 2ml for 5 min RT and then a wash was performed. Small intestines were harvested and cleaned of fat residue and Peyer's patches. To obtain lamina propria cells (LPC), the small intestine was cut longitudinally and scraped in PBS 1X to clean the mucus and faeces. The clean tissue was fragmented into pieces in 20ml HBSS 2% FCS. The pieces were filtered through a 100µm mesh and were incubated in 10ml HBSS 2mM EDTA in a shaker at 37°C for 20 min. The pieces were rinsed with HBSS through a 100µm mesh and incubated in 10ml HBSS 2mM EDTA in a shaker at 37°C for 20 min. The pieces were rinsed with HBSS, filtered through a 100µm mesh and incubated in 15 ml IMDM +10% FCS containing 1mg/ml collagenase VIII (Sigma) in a shaker at 37°C for 15 min in order to disaggregate the tissue. Single-cell suspensions were then washed and filtered (100 and 40 µm cell strainer). For T-cell re-stimulation, cells were incubated for 2h, 37°C, 5% CO₂ in RPMI 1640 supplemented with v/v 2% fetal calf serum using 1:500 Biolegend's Cell Activation Cocktail (with Brefeldin A) (Cat.No.423304) and 1:1000 Monensin Solution (1,000X) (Cat.No.420701). Staining was performed using Live/Dead discrimination by using DAPI or ZombieDyeNIR according to the manufacturer's instructions. After washing (~400g, 5min, 4°C), cells were stained in 25µl of titrated antibody master mix for 20min at 4°C and washed again (antibodies shown in **tables 2** and **3**). Samples for flow cytometric activated cell sorting (FACS) were then sorted. Samples for flow cytometry were fixed using eBioscience IC fixation

(Cat.No.00-8222-49) according to the manufacturer's instructions. Cells were analyzed using BD FACSFortessa, and data were analyzed using FlowJo. For sorting, a FACS Aria II and a FACS Aria FUSION in collaboration with the DKFZ FACS core facility were used³.

Immunoglobulin A (IgA) ELISA

96-well flat-bottom plates (Nunc) were coated by using goat anti-mouse IgA (1040-01, SouthernBiotech) as coating antibody at 4°C overnight. Plates were washed by washing buffer (0.05% Tween 20 in PBS) and blocked with 2% (w/v) BSA/PBS. Serum or homogenised tissue was loaded onto plates for 1hr room temperature incubation. Peroxidase-conjugated anti-mouse IgA α chain specific antibody (A4789, Sigma) and ABTS (Boehringer) were sequentially added as secondary antibody and substrate. IgA purified from mouse myeloma (Cat.No.553476, BD Pharmingen™) was included as a quantification standard.

Faecal IgA flow cytometry and sorting of IgA⁺ and IgA⁻ bacteria

Faecal homogenates were stained with PE-conjugated Anti-Mouse IgA (eBioscience, clone mA-6E1) prior to flow cytometric analysis and FACS sorting⁴. In detail, faecal pellets collected directly from two co-housed mice or ~100 mg of frozen murine faecal material were placed in Fast Prep Lysing Matrix D tubes containing ceramic beads (MP Biomedicals) and incubated in 1 mL Phosphate Buffered Saline (PBS) per 100 mg faecal material on ice for 1 hour. Faecal pellets were homogenized by bead beating for 5 seconds (Minibeadbeater; Biospec) and then centrifuged (50 x g, 15 min, 4°C) to remove large particles. Faecal bacteria in the supernatants were removed (100

µl/sample), washed with 1 mL PBS containing 1% (w/v) Bovine Serum Albumin (BSA, American Bioanalytical; staining buffer) and centrifuged for 5 min (8,000 x g, 4°C) before resuspension in 1 mL staining buffer. A sample of this bacterial suspension (20 µl) was saved as the Pre-sort sample for 16S sequencing analysis. After an additional wash, bacterial pellets were resuspended in 100 µl blocking buffer (staining buffer containing 20% Normal Rat Serum for mouse samples or 20% Normal Mouse Serum for human samples, both from Jackson ImmunoResearch), incubated for 20 min on ice, and then stained with 100 µl staining buffer containing PE-conjugated Anti-Mouse IgA (1:12.5; eBioscience, clone mA-6E1) for 30 minutes on ice. Samples were then washed 3 times with 1 mL staining buffer before flow cytometric analysis or cell separation. Anti-IgA-stained faecal bacteria were incubated in 1 ml staining buffer containing 50 µl Anti-PE Magnetic Activated Cell Sorting (MACS) beads (Miltenyi Biotec) (15 min at 4°C), washed twice with 1 ml Staining Buffer (10,000 x g, 5 min, 4°C), and then sorted by MACS (Possel_s program on an AutoMACS pro; Miltenyi). After MACS separation, 50 µl of the negative fraction was collected for 16S sequencing analysis (IgA negative fraction). The positive fraction was then further purified via Fluorescence Activated Cell Sorting (FACS Aria; BD Biosciences). For each sample, 2 million IgA-positive bacteria were collected, pelleted (10,000 x g, 5 min, 4°C), and frozen along with the Pre-sort and IgA-negative samples at -80°C for future use⁴.

Opt-SNE analysis

Visualization of the global single-cell landscape was performed in OMIQ using Opt-SNE based on channels IgA, CD20, and B220 for the B cells (random seed 3719, max iterations 1000, opt-SNE end 5000, perplexity 30, theta 0.5 and verbosity 25) for the B

cells pre-gated on CD45⁺liveCD19⁻. Visualization of T-cells of the global single-cell landscape was performed in OMIQ using Opt-SNE based on channels CD8 α , PD-1, and CD4 (random seed 7996, max iterations 1000, opt-SNE end 5000, perplexity 30, theta 0.5 and verbosity 25) on cells pre-gated to CD45⁺liveCD19⁻.

Histology, immunohistochemistry, scanning and automated analysis

Tissues were fixed in 4% paraformaldehyde and paraffin-embedded. For immunofluorescence staining, organs were fixed in 4% PFA for 12 hours, then transferred to 30% sucrose solution until the organs sank. Afterwards, organs were transferred into 70% EtOH before dehydration and paraffin embedding. Briefly, 2 μ m sections from formalin-fixed paraffin-embedded (FFPE) and cryo-preserved tissues were prepared and stained with Hematoxylin/Eosin or IHC antibodies (**Table S4**) on a Bond MAX (Leica). Slides were scanned with SCN400 slide scanner (Leica) and analyzed either using for area-based staining Tissue IA image analysis software by Leica Biosystems Version 4.0.6, or macro-based analysis by ImageJ, Aperio System. For Sudan red⁺ liver areas, data are presented as a percentage of total tissue area. Five random liver tissue areas of 10X zoom were selected in Aperio. NAFLD activity scoring (NAS) was performed on mouse livers³. For immunofluorescence staining, IHC-established antibodies were used, coupled by the AKOYA Biosciences Opal fluorophore kit (Opal 520 Cat.No. FP1487001KT, Opal 540 Cat.No. FP1494001KT, Opal 620 Cat.No. FP1495001KT). Confocal microscopy was performed on 30 μ m thick FFPE small intestine (ileum) sections, stained with IHC-established antibodies (**Table S4**), like previously described⁵. Briefly, antigen retrieval was performed in 1mM EDTA

ph9 0.05% tween-20 at 100°C for 20 minutes. Sections were then permeabilized and blocked in PBS containing 0.3% Triton X-100 (Sigma-Aldrich) and 10% FBS followed by staining in the same blocking buffer. Stained slides were mounted with Fluorsave (Merck Millipore) and images were acquired on an inverted Leica microscope (TCS STED CW SP8, Leica Microsystems) with a motorized stage for tiled imaging. 3D reconstruction using Imaris (Bitplane) was described previously⁵.

Murine intestine and liver single-cell RNA-Seq analysis

Sequencing output reads were converted to FASTQ files using bcl2fastq (v1.8.3) and aligned to the mm10 reference genome (2020-A version, downloaded from 10X website), using the Cell Ranger pipeline (v6.0.1, 10X Genomics). Filtered raw counts data was imported into Seurat R package (v4.0.4) (PMID: 29608179) for further processing and analysis. Raw transcript counts of gene–cell matrices were filtered to remove cells with fewer than 500 transcripts and 250 features and cells with more than 10% mitochondrial genes. In addition, genes expressed in less than 10 cells were removed from the analysis. The UMI counts matrices were then log normalized and scaled with Seurat's NormalizeData and ScaleData functions. The Seurat package was applied to identify major cell types using dimension reduction followed by clustering of cell groups. Genes with the highest variance were used to perform linear dimensional reduction (principal component analysis), and the number of principal components used in downstream analyses was chosen considering Seurat's PCHeatmap and Elbowplot. Seurat's unsupervised graph-based clustering was performed on the projected PC space. We used Seurat to perform graph-based unsupervised clustering, uniform manifold approximation and (UMAP) (McInnes, L.,

Healy, J., Saul, N. & Großberger, L. UMAP: uniform manifold approximation and projection. *J. Open Source Softw.* 3, 861 (2018)) and t-stochastic neighbour embedding (t-SNE), for data visualization in two-dimensional space. P values were calculated using one-vs.-rest Seurat's *FindAllMarkers* function configured with Wilcoxon signed-rank statistical test (two-sided test), min.pct = 0.5 and logfc.threshold=0.5. Differentially expressed genes of the clusters were used to identify cell types with help from "ImmGen – My Gene Set web tool" (http://rstats.immgen.org/MyGeneSet_New/index.html). Differentially expressed genes between the conditions within each cluster were calculated using Seurat *FindMarkers* function configured with Wilcoxon signed-rank statistical test (two-sided test), min.pct = 0.1, logfc.threshold = 0.25. Dot plots were created by modifying the output of Seurat *DotPlot* function. Violin plots and double violin plots were scattered using Seurat *VlnPlot* function.

Expression of subset of cells identified as MoMF cells (louvain clusters 1, 3, 6, 9, 17) was projected in 2D using UMAP via SCANPY⁶. Fifteen PC components were used to estimate a five-neighbour knn graph to estimate the UMAP projection. FcR γ signalling per cell was estimated with the ssgsea method implemented in the R package GSVA⁷. Distribution of mean of FCGR1 gene expression and FcR γ signalling for each sample (mouse) was plotted per diet group. Mann-Whitney U test was used to assess the significance of differential expression between control and non-control diet groups (western diet and CDA-HFD diet). SciPy 1.0 implementation of the test was used⁸. Mean expression of 496 orthologous genes that were found to be expressed in both the pre-processed human and pre-processed mouse scRNA-Seq datasets were computed for the following cell groups: SAMac, non-SAMac, MoMF and non-MoMF

cells. For each cell group the rank of the mean expression value across all genes was plotted as a clustermap using *Seaborn*.

Isolation of RNA and library preparation for bulk RNA sequencing (sorted intestinal B220+ and CD20+ cells)

300-1000 cells were sorted for each sample directly in a well (low binding Eppendorf) containing 5 μ l lysis buffer (500 μ l lysis buffer: 250 μ l of 2X TCL buffer (Qiagen, Cat.No.1070498) plus 245 μ l of RNase-free water and 5 μ l (1% of total volume) of β -mercaptoethanol). Nucleic acids of the lysates were purified with AMPure XP beads (Beckman Coulter). 1.8 volume of reagent and lysate were mixed thoroughly by pipette, followed and kept for 5 min at room temperature (RT). The mix was then placed onto Magnet Plate for 3 min to separate beads from the solution. The resulting cleared solution was aspirated from the reaction plate and discarded. Then were dispensed 150 μ l of 80% ethanol to each well; 30 sec RT, aspirated out and discarded, followed by one repetition, and let it dry for 5 min at RT. Off the magnet plate, were added 6 μ l of elution buffer (RNase-free water), pipette and mixed 10 times. On the magnet plate 1 min to separate beads from the solution. The eluate was then transferred to the retro-transcription mix for RNA-Seq processing. For the RNA-Seq, library preparation for bulk-sequencing of poly(A)-RNA was done as described previously (Parekh et al., 2016). Briefly, barcoded cDNA of each sample was generated with a Maxima RT polymerase (Thermo Fisher) using oligo-dT primer containing barcodes, unique molecular identifiers (UMIs) and an adaptor. Ends of the cDNAs were extended by a template switch oligo (TSO) and full-length cDNA was amplified with primers binding to the TSO-site and the adaptor. NEB Ultrall FS kit was used to fragment cDNA. After end repair and A-tailing a TruSeq adapter was ligated

and 3'-end-fragments were finally amplified using primers with Illumina P5 and P7 overhangs. In comparison to Parekh et al. (2016)⁹, the P5 and P7 sites were exchanged to allow sequencing of the cDNA in read1 and barcodes and UMIs in read2 to achieve better cluster recognition. The library was sequenced on a NextSeq 500 (Illumina) with 63 cycles for the cDNA in read1 and 16 cycles for the barcodes and UMIs in read2. Data were processed using the published Drop-seq pipeline (v1.0) to generate sample- and gene-wise UMI tables¹⁰. Reference genome (GRCm38) was used for alignment. Transcript and gene definitions were used according to the GENCODE Version M25.

Differential gene expression bulk transcriptomes of liver tissues and of FACS-sorted B-cells

Gene-level raw RNA-seq read counts were imported into R using the DESeq2 `DESeqDataSetFromMatrix` function¹¹. Genes with less than 10 reads across all samples were excluded from the analysis. Differential expressions between tested conditions were determined using the linear modelling approach as implemented in DESeq2, while statistical significance was accepted for absolute log₂-fold changes greater than 0.5, p-values smaller than 0.05 and false-discovery rates of smaller than 25%.

Liver CD45⁺ sorting and 10X scRNA-Seq

All experiments were performed with male C57BL6/J wildtype mice that were housed under pathogen-free conditions at the Animal Facility of the University Hospital Aachen. Livers were first perfused with 5 ml of PBS. Afterwards, livers were put in a digestion medium containing collagen-IV solution and placed in a waterbath (37°C) for 30 min. Liver cells were sorted for CD45⁺ cells (APC-Cy7), excluded B and T Cells and

Neutrophils (Table S5) in a BD FACSAria II Cell Sorter. Staining for sorting liver CD45⁺ cells (for scRNA-Seq) is reported in Table S5, and it was used Hoechst to exclude dead cells. After the isolation, the cells were washed once with cold PBS + 0.1% BSA and subjected to single-cell RNA sequencing analysis using the Chromium System (10x Genomics, California, USA). The used kits were based on v2 chemistry, using Chromium Single Cell 3' Library & Gel Bead Kit v2, and Chromium Single Cell A Chip Kit. Sequencing was performed on Illumina NextSeq 550 platform (paired-ends, 2×75 bp).

Primary cell cultures

Bone-marrow-derived macrophages (BMDMs) were derived using bone marrow from the femurs and tibias of male mice and seeded at 1.0×10^4 cells per cm^2 in Roswell Park Memorial Institute Medium (RPMI, GIBCO) containing 10% FCS (heat inactivated: 56 °C, 30min) + 1% Pen/Strep + MCSF in a final concentration of 50ng/ml. BMDMs were washed and treated in the same conditions for seven consecutive days. After eight days, in which cells had fully differentiated into macrophages, they were pre-treated with Fc block (1:100), treated with IgA (165ug/ml), and/or 3% of serum from mice fed a CD-HFD or ND, 3% of serum from mice treated with CCl₄. RNA was extracted from the cells for q-RT PCR analysis.

Chemokine dependent migration of bone-marrow derived cells

1×10^6 total bone-marrow-derived cells (isolated as described above) were cultured on 200 μl RPMI-1640 + 1% Pen/Strep + 1:200 BSA 3% together with 100 ng/ml of CCL2

chemokine (Cat.No. 250-10, PeproTech) on culture inserts into a 24-well plate. After an incubation of 37°C for 90 min, migrated cells were gently scratched from the lower side of the membrane collected. Also, migrated cells into the lower compartment of the plate were collected, washed and analysed by FACS.

Multiplex cytokine assay

Liver and serum samples from mice fed a CD-HFD, or a ND were analyzed for cytokines (IL-1 β , TNF and IL-6) using the MSD U-PLEX Biomarker Group 1 (mouse) assay according to the manufacturer's instructions.

Hydroxyproline Assay

Hepatic collagen was measured as described¹². Briefly, liver samples were hydrolyzed with 6 N HCl at 110°C for 16 hours, then filtered and mixed with methanol and evaporated by a vacuum concentrator (Eppendorf). The crystallized samples were dissolved in 50% isopropanol and incubated with 0.6% chloramine-T for 10 minutes. One hundred microliters of freshly prepared Ehrlich's reagent were added, and samples were incubated at 50°C for 45 minutes under constant shaking. Samples were measured at 570 nm, and concentrations of total liver hydroxyproline were calculated against a standard curve.

EAE (Experimental Autoimmune Encephalomyelitis) induction and scoring

Mice were injected with 50 μ g MOG₃₅₋₅₅ emulsified in complete Freund's adjuvant (CFA) supplemented with 10mg/mL heat-inactivated *Mycobacterium*

tuberculosis H37RA into the tail base. In addition, mice were intraperitoneally injected with 100 ng of pertussis toxin (PTx) on days 0 and 2. Mice were observed daily to monitor EAE clinical symptoms on a scale from 0 to 4. Daily scoring was performed using the following criteria: 0, no disease; 0.5: limb tail; 1: paralyzed tail; 1.5: weakened righting reflex; 2: no righting reflex; 3: partial paralysis of hind legs; 3.5: paralysis of one hind leg; 4: paralysis of both hind legs.

IL-2 ELISA

Splenocytes from EAE-immunized mice were collected and restimulated with 5 ug/ml MOG₃₅₋₅₅ peptide for 2 days. The culture supernatants were collected and IL-2 were measured by ELISA accordingly the manufacturer's description (BD, Cat.No. 555148).

In vitro co-culture

Single-cell suspension of small intestine (SI) lamina propria was generated as described¹³. Briefly, SI were harvested and cleaned of fat residue and Peyer's patches. To obtain lamina propria cells the small intestine was cut longitudinally and scraped in PBS 1X to clean the mucus and feces. The clean tissue was fragmented into pieces in small intestine Predigestion Medium (RPMI 1640 + GlutaMAX 1X (Gibco) supplemented with 10 mM HEPES, 5 mM EDTA, 1 mM DTT (Sigma), and 5% FBS) and incubated in a shaker at 37°C for 20 min. The supernatant was discarded and the samples were washed 4 times with PBS 1X to remove EDTA; they were subsequently incubated in SI Digestion Medium (RPMI 1640 + GlutaMAX 1X supplemented with 10 mM HEPES, 50 µg/ml DNase I (Roche), and 20 µg/ml Liberase DH (Roche)) for 27

min in a shaker at 37°C in order to disaggregate the tissue. Single-cell suspensions were then washed, and filtered (40 µm cell strainer) and the B cells were enriched with a EasySep murine B cell isolation kit (Cat.No. 19844, StemCell Technologies) according to the manufacturer's protocol. For the isolation of splenic CD8⁺ T cells, spleens were smashed (70 µm cell strainer), erythrocytes lysed with red blood cell lysis buffer and CD8⁺ T cells were enriched with Miltenyi Biotec murine CD8α⁺ T cell isolation kit (Cat.No.130-104-075) according to the manufacturer's protocol. Small intestine B cells and splenic T cells were co-cultured 1:1 in X-VIVO 15 media (Cat.No..BE02-060F, Lonza) supplemented with L-glutamine and 10% FBS in the presence of Dynabeads Mouse T-Activator CD3/CD28 (Cat.No.11456D, Thermo Fisher). OT-1 T cells were also processed using Miltenyi Biotec murine CD8α⁺ T cell isolation kit, and were co-cultured with isolated intestinal B cells (concentration 1:1) in the presence of Dynabeads.

Flow cytometry stainings of surface-expressed molecules were performed in FACS buffer containing PBS with 2mM EDTA and 2% FBS. Cell viability was assessed by staining with LIVE/DEAD Fixable Near-IR dye (Cat.No. L10119, Invitrogen). Antibodies used are listed in Table S6. For experiments with blocking antibodies, were used 10 µg/ml of anti-LFA-1α (Cat.No.BE0006-1MG, clone M17/4, BioXCell); anti-ICAM1 (Cat.No. BE0020-1, clone YN1/1.7.4, BioXCell); anti-MHCI (Cat.No. BE0077, clone M1/42.3.9.8, BioXCell). All flow cytometry analyses were performed on a BD LSRFortessa (BD Biosciences) and analyzed with FlowJo software (Treestar).

Immunohistochemistry and Immunofluorescence of human liver tissues

Human FFPE liver samples from 31 NAFLD liver biopsies were immunostained with antibodies directed against FcεR1γ (sc390222, Santa Cruz Biotechnology), S100A4 (PRB-497P, Biolegend) and CCR2 (ab176390, Abcam). Envision Flex+ reagent (Dako) was used as secondary antibody at room temperature and 3',3'-diaminobenzidine for the visualization step. Immunopositive cells in the liver biopsies were quantified in the parenchyma and the portal tracts using the Positive Cell Detection tool from QuPath vs2.3.¹⁷ In addition, portal infiltrate was assessed using a semi-quantitative score: 0=absent, 1= few cells in ≥1PT, 2= +/- one aggregate in ≥1PT, 3=aggregates in every PT.

Fluorescent double staining was performed on a selection of 6 human NAFLD FFPE biopsy samples using antibodies against FcεR1γ (sc390222, Santa Cruz Biotechnology), S100A4 (PRB-497P, Biolegend) and CD163 (ab182422, Abcam). Goat anti-mouse Alexa Fluor 488 and Goat anti-rabbit Alexa Fluor 594 were used as secondary antibodies (Invitrogen™/Thermo Fisher Scientific). Nuclear counterstaining was performed using 4',6-diamidino-2-phenylindole (Invitrogen™). Slides were analyzed using the Leica TCS SP8 confocal microscope platform (Leica Microsystems).

Human bulk liver transcriptome analysis

For bulk liver transcriptome heatmap visualization (NASH F0-F4 versus NAFL) Fastqc (v0.11.5) and MultiQC (v1.2dev) were used for raw sequencing quality assessment and alignment to the reference genome (GRCh38, Ensembl release 76). Gene-level count tables were produced using HT-Seq. Trimmed mean of M values method was

used to normalize counts and limma's voom methodology for transformation. A correction for sex, batch and centre effect was implemented.

Single-cell RNA-Seq analysis of CD45⁺ cells from human livers

The scRNA-Seq data of the immune cells from healthy donors (n=5) and from cirrhotic patients (n=5) which were part of the study of Ramachandran et al. (2019)¹⁸, and from unpublished data (1 cirrhotic patient), of which were provided as an R-Seurat v2 object. The object which contained detailed annotation of immune cell types was converted to an h5ad Annotated Dataframe object before importing into a Python environment. The newly generated data from another healthy donor was also imported. The two datasets were independently preprocessed using SCANPY (1.8.2)⁶ which included count normalization per cell, filtering out cells with less than 200 genes expressed and excluding genes which were detected in less than 3 cells. The two data sets (z-scaled) were integrated using the SCANPY ingest method in which immune cell annotations of cells of the new dataset were learnt from the ground-truth annotation ("annotation_indepth") of the Ramachandran et al. (2019) data set. Two-dimensional UMAP (Uniform Manifold Approximation and Projection) plots based on neighbourhood graphs were generated for topological representation of cell transcriptomes in relation to immune cell annotations. FC-gamma-receptor pathway activity was inferred from scRNA-Seq counts using R GSVA⁷ executed using Python rmagic (rpy). The Mann-Withey U test was applied to the per-sample averaged values for gene expression or pathway activity to statistically test for differences between groups.

Patient selection

845 cases were derived from the European NAFLD Registry (NCT04442334)¹⁴. These included 639 cases with histologically characterized NAFLD for whom serum IgA levels measured during routine clinical management were available, recruited from the Freeman Hospital, Newcastle Hospitals NHS Foundation Trust, Newcastle-upon-Tyne, UK. Liver tissue samples were scored according to the semi-quantitative NASH-CRN Scoring System¹⁵. Patient samples were grouped according to disease activity and stage: non-alcoholic fatty liver and non-alcoholic steatohepatitis (NASH) with different stages of fibrosis (F0 to F4). Alternate diagnoses and etiologies, such as excessive alcohol intake, viral hepatitis, and autoimmune liver diseases, were excluded. A subset of 54 cases was used for immunohistochemistry and/or immunofluorescence as described above, of which clinical features are listed in **Table S7**. In addition, RNA sequencing analysis was performed using the data from 206 snap-frozen biopsy samples from 206 patients diagnosed with NAFLD from France, Germany, Italy and the UK (GSE135251)¹⁶. This study was approved by the relevant Ethical Committees in the participating countries. Jejenum human samples were collected from the hospital of Mannheim (ethical number 2012-293N-MA), and of Würzburg (ethical permits 96/12 and 188/17).

Statistical analyses

Mouse data are presented as the mean \pm SEM. Pilot experiments and previously published results were used to estimate the sample size, such that appropriate statistical tests could yield significant results¹⁹. Statistical analysis was performed using

GraphPad Prism software version 9.3 (GraphPad Software). Exact p-values lower than $p < 0.1$ are reported and specific tests are indicated in the legends.

Supplementary tables

Table S1. Murine primer sequences for qRT-PCR

Gene	Primer sequence
mAbca1 fwd	GTT TTG GAG ATG GTT ATA CAA TAG TTG T
mAbca1 rev	TTC CCG GAA ACG CAA GTC
mAcad10 fwd	TGG CTG TGG GCT GGG AG
mAcad10 rev	AAA TAG GAG CTG ACG GGC AC
mAcat2 fwd	GAC CCC GTG GTC ATC GTC
mAcat2 rev	CCA CAA CCT GCC GTC AAG A
mAcat3 fwd	TGG CCA CTT TGA CAA GGA GAT
mAcat3 rev	CTGTTGCATTAGCAGTTGTGA
mAcot2 fwd	CTC GTC TTT CGC TGT CCT GA
mAcot2 rev	CTC AGC GTC GCA TTT GTC CG
mAcox3 fwd	GGG TGA TGG TCG GTG ACA TT
mAcox3 rev	CGG ACA TCC TTA AAG GGG CT
mAcsbg1 fwd	ACT CGC AAA CCA GCT CC
mAcsbg1 rev	AGT ACA GAA AGG TTC CAG GCG
mAcsl1 fwd	ATC TGG TGG AAC GAG GCA AG
mAcsl1 rev	TCC TTT GGG GTT GCC TGT AG
mAcsm2 fwd	GCC AGA CAG AAA CGG GAC TT
mAcsm2 rev	ACA TGC CGA TAG GCC AGA TG
mCcl5 fwd	TTA GCC TAG ATC TCC CTC G
mCcl5 rev	CGA CTG CAA GAT TGG AGC ACT
mCol1a1 fwd	ACG CAT GAG CCG AAG CTA AC
mCol1a1 rev	TTG GGG ACC CTT AGG CCA TT
mCol6a1 fwd	CCC CTG GAG AGA GGG GTG GC
mCol6a1 rev	CCG GGG AAA CCT TCC GTG CC
mCxcl1 rev	AGT GTG GCT ATG ACT TCG GTT
mCxcl1 fwd	GCC TCT AAC CAG TTC CAG CA
mEl fwd	CTA TCC CAA TGG CGG TGA CTT C
mEl rev	CGT GCT CGC ATT TCA CCA TC
mFmod fwd	TCC AAC CCA AGG AGA CCA GA
mFmod rev	GGT CGT AGT AGG TGG ACT GC
mGpat fwd	GCT GCA ACT GAG ACG AAC CT
mGpat rev	AAG CCC CCA AGC TTG TGA AT
mHl fwd	CTA TGG CTG GAG GAA TCT G
mHl rev	TGG CAT CAT CAG GAG AAA G

Gene	Primer sequence
mL-1b fwd	TCC CGT GGA CCT TCC AGG ATG A
mL-1b rev	GGG AAC GTC ACA CAC CAG CAG G
mL-6 fwd	CTC TGG AGC CCA CCA AGA AC
mL-6 rev	GTC ACC AGC ATC AGT CCC AA
mLgals1 fwd	CTC AAA GTT CGG GGA GAG GTG
mLgals1 rev	AGC GAG GAT TGA AGT GTA GGC
mLgals3 fwd	TAA TCA GGT GAG CGG CAC AG
mLgals3 rev	CCA GAG CCA GCT AAG GCA TC
mLipe fwd	CTT CCA GTT ACC TGC CA
mLipe rev	AAT CGG CCA CCG GTA AAG AG
mLum fwd	TGA ACT GGC TGA TAG TGG GG
mLum rev	GAG TAA GAC AGT GGT CCC AGG
mMvd fwd	GAG GGA GAC CTC TCC GAA GT
mMvd rev	GTC TGC ARG CCC ACT GTA CT
mPdgr1a fwd	TGG CAT GAT GGT CGA TTC TA
mPdgr1a rev	CGC TGA GGT GGT AGA AGG AG
mPpard fwd	GAA CAG CCA CAG GAG GAG AC
mPpard rev	GAG GAA GGG GAG GAA TTC TG
mS100a4 fwd	CAC TTC CTC TCT CTT GGT CTG
mS100a4 rev	AAC TTG TCA CCC TCT TTG CC
mSpp1 fwd	ATG AGG CTG CAG TTC TCC TGG
mSpp1 rev	GCC AAA CAG GCA AAA GCA AAT C
mSqle fwd	GCA ATC TAC GCC ACG TAT TTC T
mSqle rev	GGG CCC GTG GTT TTG T
mTgfb1 fwd	GGA GCA ACA TGT GGA ACT C
mTgfb1 rev	CAG CAG CCG GTT ACC AAG
mTnfa fwd	CGA TGG GTT GTA CCT TGT C
mTnfa rev	CGG ACT CCG CAA AGT CTA AG
mTrem2 rev	GAA AGA GGA GGA AGG TGG TAG GC
mTrem2 fwd	AGG TCC TGC AGA AAG TAC TGG T
Pdgfbr fwd	GCT CCG TCT ACG CGT CC
Pdgfbr rev	GAA TGG GAT CCC CCT CGG
Tgfb1 fwd	GGA GCA ACA TGT GGA ACT C
Tgfb1 rev	CAG CAG CCG GTT ACC AAG

Table S2. Flow cytometry antibodies used for murine intestine experiments

Small Intestine - flow cytometry antibodies				
Marker	Fluorochrome	Clone	Ordering #	Company
CD44	Brilliant Violet 421™	IM7	103039	Biolegend
CXCR4	Brilliant Violet 421™	L276F12	146511	
LIVE/DEAD	Brilliant Violet 510™		423102	
PD-1(CD279)	Brilliant Violet 605™	29f.1a12	135220	
CD4	Brilliant Violet 650™	GK1.5	100469	
B220	Brilliant Violet 650™	RA3-6B2	103241	
IgA	FITC	C10-3	559354	BD Pharmingen™
CD20	PE	SA271G2	152105	Biolegend
CD69	PE	H1.2F3	104508	
IgM	PE	RMM-1	406507	
CD45	PE/Cyanine5	30-F11	103110	
CD19	PE/Cyanine7	6D5	115520	
CD20	PE/Cyanine7	SA275A11	150419	
CD62L	PE/Dazzle™	MEL-14	104448	
IgD	PE/Dazzle™	11-26c.2a	405741	
CD8 α	PerCP/Cyanine5.5	53-6.7	100734	
MHC-II	PerCP/Cyanine5.6	M5/114.15.2	107625	

Table S3. Flow cytometry antibodies used for murine liver experiments

Liver - flow cytometry antibodies					
Marker	Fluorochrome	Clone	Ordering #	Company	
CD4	Alexa Fluor® 700	RM4-5	100536	Biolegend	
CD45		30-F11	103128		
MHC-II		M5/114.15.2	107622		
CD11b	APC	M1/70	101212		
CD3		17A2	100236		
CD44		IM7	103012		
IFN- γ		XMG1.2	505810		
CD19	APC/Cyanine7	6D5	115530		
LIVE/DEAD			423106		
CD3	Brilliant Violet 421™	17A2	100228		
CD45R/B220	Brilliant Violet 650™	RA3-6B2	103241		
CD45	Brilliant Violet 785™	30-F11	103149		
CD19	FITC	6D5	115505		
CD45		I3/2.3	147710		
CD69	PE	H1.2F3	104508		
F4/80		BM8	123110		
Perforin		s16009a	154306		
CD3	PE/Cyanine7	17A2	100220		
Ly6G		1A8	127618		
CSF-1R(CD115)	PE/Dazzle™	AFS98	135527		
CD11c		N418	117348		
CD62L		MEL-14	104448		
TNF		MP6-XT22	506346		
CD8a	PerCP/Cy5.5	53-6.7	100734		
Ly6C		HK1.4	128011		
CD16/32	-	93	101302		
LIVE/DEAD	AmCyan		L34966		Thermo Fischer Scientific

Table S4. IHC primary antibodies anti-mouse

Antibody	Clone	Ordering #	Company
B220	RA3-6B2	553084	BD Biosciences
B220-Alexa Fluor®647	RA3-6B2	103226	Biolegend
CD11b	EPR1344	ab133357	Abcam
CD3	SP7	ab16669	Abcam
CD8	4SM15	14-0808-82	Invitrogen
CD8α-Alexa Fluor®488	EPR21769	ab237364	Abcam
Cleaved Caspase 3 (Asp175)	polyclonal	9661	Cell Signaling
Collagen type IV	CL50451AP-1	CL50451AP-1	Cedarlane
EpCAM-Brilliant Violet 421™	G8.8	118225	Biolegend
F4/80	BM8	123105	BioLegend
FCER1G	polyclonal	PA5-109716	Invitrogen (Thermo Fisher Scientific)
FCGR1	1	50086-R001	Sino Biological
Gp73	F-2	sc-365817	Santa Cruz Biotechnology
IgA	M18-254	553476	BD Pharmingen™
IgM	polyclonal	A 0425	DAKO
Ki67	SP6	RM-9106-S1	Thermo Fisher Scientific
Ly6C	ER-MP20	ab15627	Abcam
MHCII	M5/114.15.2	NBP1-43312	Novus Biologicals
P62	polyclonal	MBL-PM045	Biozol diagnostica
PDGFRβ	28E1	3169s	Cell Signaling Technology
Phospho-HCK(Tyr411)	polyclonal	orb184018	Biorbyt
Phospho-SYK(Tyr525)	polyclonal	PA5104904	Invitrogen (Thermo Fisher Scientific)
S100A4	polyclonal	810101	BioLegend

Table S5. Flow cytometry antibodies used for murine liver CD45⁺ sorted cells for subsequent scRNA-Seq

Liver CD45 ⁺ sorted cells for scRNA-Seq - flow cytometry antibodies				
Marker	Fluorochrome	Clone	Ordering #	Company
CD3e	Alexa Fluor® 488	145-2C11	557666	BD Pharmingen™
CD45	APC/Cyanine7	30-F11	557659	
CD19	FITC	1D3	553785	
NK1.1	PE	PK1136	553165	
Ly6G		1A8	551461	
TCRγδ		GL-3	12-5711-82	
CD4	PE/Cyanine7	RM4-5	12-0042-83	eBioscience™
TCRβ		H57-597	25-5961-82	
Hoechst 33258	eFluor™ 450	-	94403	Sigma-Aldrich

Table S6. Flow cytometry antibodies used for co-culture experiments with intestinal B cells and T cells

Co-culture small intestine anti-mouse flow cytometry antibodies				
Marker	Fluorochrome	Clone	Ordering #	Company
CD8α	APC	53-6.7	100712	Biolegend
CD25	PE	PC61.5	12-0251-81	eBioscience™
CD152 (CTLA-4)	PE/Cyanine7	UC10-4B9	25-1522-82	eBioscience™
CD279 (PD-1)	BUV737	RMP1-30	749306	BD Bioscience
CD69	FITC	H1.2F3	104506	Biolegend
CD186 (CXCR6)	Brilliant Violet 421™	SA051D1	151109	Biolegend
CD19	PerCP/Cyanine5.5	1D3	45-0193-82	eBioscience™
CD45R/B220	Brilliant Violet 711™	RA3-6B2	103255	Biolegend

Table S7. Patient clinical features of analysed histological samples (liver and jejunum)

Clinical features	N total (n= 54)	Count/mean ± SD
Age (mean ± SD)	54	50.6 ± 10.9
Sex	54	
Male		28
Female		26
BMI (mean ± SD)	51	40.3 ± 7.7
ALT (mean ± SD)	35	49.1 ± 28.7
NAS (mean ± SD)	53	3.5 ± 1.8
NAS score ≤ 2		16
NAS score ≥ 3		37
Fibrosis (mean ± SD)	51	1.8 ± 1.5
Fibrosis score (Kleiner) ≤ F2		30
Fibrosis score (Kleiner) F3/F4		21

Supplementary references

Author names in bold designate shared co-first authorship.

1. Tomura M, Yoshida N, Tanaka J, et al. Monitoring cellular movement in vivo with photoconvertible fluorescence protein "Kaede" transgenic mice. *Proc Natl Acad Sci U S A*. Aug 05 2008;105(31):10871-6. doi:10.1073/pnas.0802278105
2. Krebs CF, Paust HJ, Krohn S, et al. Autoimmune Renal Disease Is Exacerbated by S1P-Receptor-1-Dependent Intestinal Th17 Cell Migration to the Kidney. *Immunity*. 11 15 2016;45(5):1078-1092. doi:10.1016/j.immuni.2016.10.020
3. Pfister D, Núñez NG, Pinyol R, et al. NASH limits anti-tumour surveillance in immunotherapy-treated HCC. *Nature*. Apr 2021;592(7854):450-456. doi:10.1038/s41586-021-03362-0
4. Palm NW, de Zoete MR, Cullen TW, et al. Immunoglobulin A coating identifies colitogenic bacteria in inflammatory bowel disease. *Cell*. Aug 28 2014;158(5):1000-1010. doi:10.1016/j.cell.2014.08.006
5. Malehmir M, Pfister D, Gallage S, et al. Platelet GPIb α is a mediator and potential interventional target for NASH and subsequent liver cancer. *Nat Med*. 04 2019;25(4):641-655. doi:10.1038/s41591-019-0379-5
6. Wolf FA, Angerer P, Theis FJ. SCANPY: large-scale single-cell gene expression data analysis. *Genome Biol*. 02 06 2018;19(1):15. doi:10.1186/s13059-017-1382-0
7. Hänzelmann S, Castelo R, Guinney J. GSEA: gene set variation analysis for microarray and RNA-seq data. *BMC Bioinformatics*. Jan 16 2013;14:7. doi:10.1186/1471-2105-14-7
8. Virtanen P, Gommers R, Oliphant TE, et al. SciPy 1.0: fundamental algorithms for scientific computing in Python. *Nat Methods*. 03 2020;17(3):261-272. doi:10.1038/s41592-019-0686-2
9. Parekh S, Ziegenhain C, Vieth B, Enard W, Hellmann I. The impact of amplification on differential expression analyses by RNA-seq. *Sci Rep*. 05 09 2016;6:25533. doi:10.1038/srep25533
10. Macosko EZ, Basu A, Satija R, et al. Highly Parallel Genome-wide Expression Profiling of Individual Cells Using Nanoliter Droplets. *Cell*. May 21 2015;161(5):1202-1214. doi:10.1016/j.cell.2015.05.002
11. Love MI, Huber W, Anders S. Moderated estimation of fold change and dispersion for RNA-seq data with DESeq2. *Genome Biol*. 2014;15(12):550. doi:10.1186/s13059-014-0550-8

12. Heymann F, Hammerich L, Storch D, et al. Hepatic macrophage migration and differentiation critical for liver fibrosis is mediated by the chemokine receptor C-C motif chemokine receptor 8 in mice. *Hepatology*. Mar 2012;55(3):898-909. doi:10.1002/hep.24764
13. Valle-Noguera A, Gómez-Sánchez MJ, Girard-Madoux MJH, Cruz-Adalia A. Optimized Protocol for Characterization of Mouse Gut Innate Lymphoid Cells. *Front Immunol*. 2020;11:563414. doi:10.3389/fimmu.2020.563414
14. Hardy T, Wonders K, Younes R, et al. The European NAFLD Registry: A real-world longitudinal cohort study of nonalcoholic fatty liver disease. *Contemp Clin Trials*. Oct 9 2020;98:106175. doi:10.1016/j.cct.2020.106175
15. Kleiner DE, Brunt EM, Van Natta M, et al. Design and validation of a histological scoring system for nonalcoholic fatty liver disease. *Hepatology*. Jun 2005;41(6):1313-21. doi:10.1002/hep.20701
16. Govaere O, Cockell S, Tiniakos D, et al. Transcriptomic profiling across the nonalcoholic fatty liver disease spectrum reveals gene signatures for steatohepatitis and fibrosis. *Sci Transl Med*. Dec 2 2020;12(572)doi:10.1126/scitranslmed.aba4448
17. Bankhead P, Loughrey MB, Fernandez JA, et al. QuPath: Open source software for digital pathology image analysis. *Sci Rep*. Dec 4 2017;7(1):16878. doi:10.1038/s41598-017-17204-5
18. Ramachandran P, Dobie R, Wilson-Kanamori JR, et al. Resolving the fibrotic niche of human liver cirrhosis at single-cell level. *Nature*. 11 2019;575(7783):512-518. doi:10.1038/s41586-019-1631-3
19. Valle JW, Borbath I, Khan SA, et al. Biliary cancer: ESMO Clinical Practice Guidelines for diagnosis, treatment and follow-up. *Ann Oncol*. Sep 2016;27(suppl 5):v28-v37. doi:10.1093/annonc/mdw324

Supplementary figure legends

Fig. S1: B-cells deficiency and therapeutic B-cells depletion avoid hepatic immune cells activation and metabolic deregulation

(A) Summary Table Sindicating clinical data as follows: serological ALT values, cholesterol, hepatic triglycerides, NAS and phenotypic outcome for WT ND, CD-HFD and JH^{-/-} CD-HFD mice. Unpaired T-test statistical analysis for: a) WT CD-HFD vs WT ND; b) JH^{-/-} CD-HFD vs WT CD-HFD; and JH^{-/-} CD-HFD vs WT ND (n≥4). **(B)** Weight development in male WT ND, CD-HFD and JH^{-/-} CD-HFD mice (n=20). **(C)** Glucose tolerance test performed in WT ND, CD-HFD and JH^{-/-} CD-HFD 9-month-old male mice (n=6). **(D)** Representative IHC for B220, CD3, F4/80, MHCII, P62, cleaved caspase 3, and PD1 quantification of the respective cells per mm² on liver sections of 6-month-old WT ND, CD-HFD and JH^{-/-} CD-HFD (n=6). **(E)** Absolute quantification of flow cytometric analyses comparing 6-month-old WT ND, CD-HFD and JH^{-/-} CD-HFD male mice (n=5) for hepatic CD3⁺ cells and CD8⁺ cells; and of **(F)** CD19⁺ cells. **(G)** Clinical data summary Table Sfor 12-month WT ND, CD-HFD and JH^{-/-} CD-HFD fed mice (n≥4). **(H)** Representative H&E liver sections of 12-month fed mice. **(I)** Clinical data summary Table Sfor controls and anti-CD20 treatment in WT CDHFD mice. Unpaired T-test statistical analysis for: a) WT CD-HFD vs WT ND; b) αCD20 CD-HFD vs WT CD-HFD; and αCD20 CD-HFD vs WT ND (n≥4). **(J)** Representative H&E staining of liver sections of 4-month (start of the depletion treatment) WT CD-HFD mice. **(K)** NAS evaluation on liver sections of 4-month WT CD-HFD mice (n=3). **(L)** Body weight of 6-month WT ND, control and αCD20-treated WT CD-HFD male mice (n=5). **(M)** Glucose tolerance test performed in 6-month male mice (n=5). **(N-P)** Absolute quantifications of flow cytometric analyses comparing control and αCD20-treated WT CD-HFD male mice (n≥3) of **(N)** spleen CD19⁺ and CD20⁺ cells, **(O)** blood CD19⁺ and CD20⁺ cells, **(P)** liver CD3⁺ cells and liver CD8⁺ cells. **(Q)** Representative liver IHC staining for B220, CD3, F4/80, MHCII and P62 quantification of the respective cells per mm² on liver sections of 6-month-old WT ND, WT CD-

HFD and α CD20-treated WT CD-HFD mice (n=6). **(R)** Real-time PCR analysis for lipid metabolism genes on mRNA isolated from WT ND and CD-HFD and $JH^{-/-}$ CD-HFD livers (n=6). **(S)** Heatmap representing hierarchical clustering analysis of lipid metabolites significantly altered (autoscaled abundance), as evaluated in male mice (n \geq 3). All data are presented as mean \pm SEM. Statistical analyses were performed using unpaired T-test or ANOVA. Displayed scale bar represents 100 μ m.

Fig. S2: Intestinal B-cells suffice to induce hepatic inflammation and metabolic dysregulation.

(A) Summary Table Summarizing clinical data as follows: serological ALT values, cholesterol, hepatic triglycerides, NAS and phenotypic outcome for WT ND, CD-HFD and μ MT CD-HFD mice. Unpaired T-test statistical analysis for: a) WT CD-HFD vs WT ND; b) μ MT CD-HFD vs WT CD-HFD; and μ MT CD-HFD vs WT ND (n \geq 4). **(B)** Weight development in male WT ND, CD-HFD and μ MT CD-HFD mice (n=20). **(C)** Glucose tolerance test performed in WT ND, CD-HFD and μ MT CD-HFD 6-month-old male mice (n=6). **(D)** Representative Ki67 staining on spleen sections of WT and μ MT CD-HFD male mice. **(E)** Quantifications of flow cytometric analyses showing percentages of small intestine lamina propria CD20⁺ and IgA⁺ cells, comparing μ MT and $JH^{-/-}$ CD-HFD mice (n=4). **(F)** Representative B220 staining on spleen sections of WT and μ MT CD-HFD male mice. **(G)** Representative IgA staining of small intestine sections of 6-month μ MT CD-HFD male mouse (upper row: scale bar 200 μ m, bottom row scale bar: 100 μ m). **(H)** IgM and IgG2b levels of small intestinal tissues measured by E.L.I.S.A. in WT ND, and in WT, $JH^{-/-}$ and μ MT CD-HFD male mice. **(I, J)** Percentages of CD19⁺, B220⁺ and IgA⁺ cells, of **(I)** caecum and **(J)** colon (n=3). **(K)** Percentages of IgA⁺ coated bacteria from faecal homogenates of WT ND and WT, $JH^{-/-}$ and μ MT mice on CD-HFD for 6 months. **(L)** Representative IHC images for B220, CD3, F4/80 and MHCII on liver sections of 6-month-old

WT ND, WT CD-HFD and μ MT CD-HFD and quantification of the respective cells per mm^2 (n=6). **(M)** Quantifications of liver flow cytometric analyses comparing 6-month WT ND, CD-HFD and μ MT CD-HFD male mice for CD3^+ and CD8^+ cells (n=4). **(N)** Real-time PCR analysis for lipid metabolism genes on mRNA isolated from WT ND and CD-HFD and μ MT CD-HFD livers (n=4). **(O)** Clinical data summary Table Sfor 12-month WT ND and WT CD-HFD mice and for μ MT CDHFD mice. Unpaired T-test statistical analysis for: a) WT CD-HFD vs WT ND; b) μ MT CD-HFD vs WT CD-HFD; and μ MT CD-HFD vs WT ND (n \geq 4). **(P)** Representative H&E staining of liver sections derived from 12-month-old WT and μ MT male mice. **(Q)** Treatment scheme for the B-cell depleted μ MT CD-HFD male mice (n=5). **(R)** Representative H&E staining of liver sections and NAS evaluation of 4-month WT and μ MT CD-HFD male mice (n=3). **(S)** Clinical data summary Table Sfor controls and for anti-CD20 treatment in μ MT CDHFD mice. Unpaired T-test statistical analysis for: a) WT CD-HFD vs WT ND; b) α CD20 μ MT CD-HFD vs WT CD-HFD; and α CD20 μ MT CD-HFD vs WT ND (n \geq 4). **(T)** Body weight values at 6-month time point of μ MT CD-HFD and of α CD20-treated μ MT CD-HFD mice. **(U)** Normalized to Mode histogram showing $\text{CD20}^+\text{IgA}^+$ cells in small intestine lamina propria of μ MT CD-HFD and μ MT CD-HFD α CD20-treated mice. **(V)** Upper panel, representative IHC images and quantifications per mm^2 on liver sections of μ MT CD-HFD and μ MT CD-HFD α CD20-treated livers; lower panel quantification of the respective cells per mm^2 for CD3, F4/80, MHCII, P62 and cleaved caspase 3 (n \geq 4). **(W)** Absolute quantifications of liver flow cytometric analyses comparing μ MT CD-HFD and μ MT CD-HFD α CD20-treated, for CD3^+ and for CD8^+ cells (n \geq 4). All data are presented as mean \pm SEM. Statistical analyses were performed using unpaired T-test or ANOVA. Displayed scale bar represents 100 μm .

Fig. S3: Intestinal B-cells are hyperactivated in NASH and require antigen presentation receptors to drive the disease.

All data represent small intestine. **(A-H)** Percentages of liver flow cytometric analysis of WT ND, WT CD-HFD and in μ MT CD-HFD mice ($n \geq 4$): **(A)** $CD20^+CXCR4^+$ cells, **(B)** IgA^+ cells, **(C)** $IgA^+B220^-CD20^-CXCR4^-$ cells, **(D)** $CD8^+CD44^+$ cells, **(E)** $CD8^+PD1^+$ cells, all of $CD45^+$ cells. **(G, H)** Percentages of $CD44^+$ cells or $PD1^+$ cells of $CD8^+$ T cells. **(I)** Representative high-resolution confocal microscopy and 3D reconstruction images of small intestine lamina propria staining for $B220^+$ and $CD8^+$ cells, and **(J)** quantification of clusters found in villi of $B220^+/CD8^+$ interacting cells, of WT ND and WT CD-HFD mice ($n=3$, with $n=8$ FOV each mouse). **(K)** Heatmaps showing Z-scores of common genes significantly deregulated in WT ND, WT CD-HFD and μ MT CD-HFD male mice RNA-Seq analysis of small intestine lamina propria $CD20^+$ sorted cells (on the right), involved in immune network for IgA production, B-cell activation and differentiation, metabolic process ($n \geq 4$). **(L)** Heatmaps displaying common genes from intestinal $B220^+$ sorted cells RNA-Seq involved in the immune system and metabolic process ($n=3$). **(M)** Flow cytometry analysis of activated $CD8^+$ cells after in vitro co-culture of isolated intestinal B cells from WT ND or WT CD-HFD with OT-1 T cells ($n=4$).

All data are presented as mean \pm SEM. Statistical analyses were performed using unpaired T-test or ANOVA. Displayed scale bar represents 100 μ m.

Fig. S4: Mouse model for absent secretion of immunoglobulin displays normal B-cells response but does not form clusters with T-cells in small intestine.

(A) Disease score measure for 16-days of Experimental Autoimmune Encephalomyelitis (EAE) in WT control and IgMi mice. **(B)** Splenic interleukin-2 levels (pg/ml) after EAE-immunization with MOG₃₅₋₅₅ or with medium as control, of WT and IgMi mice ($n=3$). **(C)** Summary Table Summarizing clinical data as follows: serological ALT values, cholesterol, hepatic triglycerides, NAS and phenotypic outcome for WT ND, CD-HFD and IgMi CD-HFD mice. Unpaired T-test statistical analysis for: a) WT CD-HFD vs WT ND; b) IgMi CD-HFD vs WT CD-HFD; and IgMi CD-HFD vs WT ND ($n \geq 4$). **(D)** On the left, representative IHC images for B220, CD3, F4/80,

MHCII, P62 and cleaved caspase 3 staining; on the right, their quantification for WT ND, WT CD-HFD and IgMi CD-HFD groups (n≥5). **(E)** Liver flow cytometric analyses displaying quantifications of liver total CD3⁺ cells or total CD8⁺ cells of WT ND, WT CD-HFD and IgMi CD-HFD groups (n=5). **(F)** High-resolution confocal microscopy images of small intestine lamina propria staining for B220⁺ cells and CD8⁺ cells and quantification of B220⁺/CD8⁺ interacting cells forming clusters in villi of WT controls and IgMi CD-HFD mice small intestines. **(G)** Representative IHC images and quantification of small intestine pospho-SYK positive immune cells (per mm²) (n≥3). All data are presented as mean ± SEM. Statistical analyses were performed using unpaired T-test. Displayed scale bar represents 100 μm.

Fig. S5: Increase of profibrogenic MoMFs is CD-HFD specific and requires FcR signalling

(A) Sirius red staining quantification from livers of 6-months WT ND and JH^{-/-}, WT αCD20-treated, μMT, IgMi, AIDg23s mice under CD-HFD (n≥4). **(B)** Representative collagen-IV stained liver sections of the groups mentioned above. **(C)** PDGFRβ staining on liver sections of the aforementioned mouse groups, with the corresponding quantification per mm² (n≥4). **(D)** Representative Sirius red (upper row) staining and quantification, and collagen-IV (bottom row) staining on liver sections for 6-months WT, μMT αCD20-treated, IgA^{-/-} and AID^{-/-} mice under CD-HFD (n≥4). **(E)** IgA serological levels (μg/ml) measured via E.L.I.S.A in 6-months WT ND and JH^{-/-}, WT αCD20-treated, μMT, IgMi, AIDg23s under CD-HFD (n≥4). **(F)** On the left, IgA serological levels (μg/ml) were measured via E.L.I.S.A in 6-months WT, μMT αCD20-treated, IgA^{-/-} and AID^{-/-} mice under CD-HFD (n≥4). On the right, correlation plot indicating serological IgA and Sirius red positivity in WT, IgA^{-/-} and AID^{-/-} mice under CD-HFD. **(G)** Real-time PCR analysis for fibrosis-related genes on mRNA isolated from 6-month WT ND and JH^{-/-}, μMT, WT αCD20-treated, AIDg23s, IgMi, and FcRγ^{-/-} mice under CD-HFD (n≥2). Statistical analysis of qRT-PCR heatmap, indicating in black asterisks the significance of groups under CD-HD

versus WT ND, and in green asterisks, the significance of groups under CD-HD versus WT CD-HFD. **(H)** Hydroxyproline levels ($\mu\text{g/g}$) of livers from 6-month WT ND and μMT , WT αCD20 -treated, AIDg23s, IgMi, and $\text{FcR}\gamma^{-/-}$ mice under CD-HFD ($n\geq 3$). **(I)** Summary Table Indicating clinical data as follows: serological ALT values, cholesterol, hepatic triglycerides, NAS and phenotypic outcome for WT CD-HFD and $\text{FcR}\gamma^{-/-}$ CD-HFD mice. Unpaired T-test statistical analysis for: a) $\text{FcR}\gamma^{-/-}$ CD-HFD vs. WT CD-HFD ($n\geq 4$). **(J)** Representative Sudan red staining of liver sections and hepatic triglycerides quantification of WT and $\text{FcR}\gamma^{-/-}$ on CD-HFD mice ($n=5$). **(K)** Liver flow cytometry analysis quantifications of total CD3^+ and CD19^+ cell populations, CD8^+ cells, $\text{CD8}^+\text{CD62L}^+$ and $\text{CD8}^+\text{CD62L}^-$ cells, $\text{CD8}^+\text{TNF}^+$ cells, $\text{CD8}^+\text{IFN}\gamma^+$ cells. **(L)** Representative IHC images of liver sections per mm^2 and quantifications for CD3, B220, F4/80 and MHCII staining of WT and $\text{FcR}\gamma^{-/-}$ on CD-HFD mice ($n=4$). **(M)** Representative IHC images of Ly6C staining or **(N)** S100A4 staining of liver sections and quantification of positive cells per mm^2 for WT ND and WT, WT αCD20 -treated, μMT , AIDg23s and $\text{FcR}\gamma^{-/-}$ mice under CD-HFD ($n\geq 3$). **(O)** Treatment scheme for the *in vitro* experiments using 12-weeks WT male mice-isolated BMDMs treated with serum of 6-month WT ND/ fibrotic WT CD-HFD/ μMT CD-HFD mice; in addition is displayed the treatment with fibrotic WT CD-HFD serum on 12-weeks $\text{FcR}\gamma^{-/-}$ male mice-isolated BMDMs. **(P)** Treatment scheme for the CCl_4 experiments with one-dose injection and sacrificing mice after 36 hours. The harvested livers were analyzed by flow cytometry, and the isolated BMDMs were used for transmigration *in vitro* assay using CCL2 cytokine and subsequent flow cytometry experiments. **(Q)** Flow cytometric analysis quantification for absolute number and percentages of $\text{CD45}^+\text{Ly6G}^-\text{Cd11c}^-\text{F4/80}^+\text{CD11b}^+\text{Ly6C}^+$, of transmigrated cells treated or not with CCL2, from BMDMs isolated from WT or $\text{FcR}\gamma^{-/-}$ mice ($n=4$), with or without CCl_4 treatment. **(R)** Absolute quantification of hepatic $\text{CD45}^+\text{Ly6G}^-\text{Cd11c}^-\text{F4/80}^+\text{CD11b}^+\text{Ly6C}^+$ of WT or $\text{FcR}\gamma^{-/-}$ mice treated or not with CCl_4 . **(S)** Measured CCL2 levels (pg/ml) livers and sera of 6-months WT ND, WT CD-HFD, μMT CD-

HFD, AIDg23s CD-HFD and $FcR\gamma^{-/-}$ CD-HFD mice. **(S)** Representative H&E, Sirius red staining, and NAS evaluation of liver section from 5-month-old male mice under ND, WD or CDA-HFD (n=4). Serological IgA values ($\mu\text{g/ml}$) (n \geq 4). **(T)** Values of mRNA expression levels of MoMFs markers in scRNA-Seq 10X analysis. **(U)** On the left, values of mRNA expression levels of genes involved in $FcR\gamma$ signalling; on the right, MoMFs clusters visualization UMAP plots (in ND, WD and CDA-HFD) and plot indicating $FcR\gamma$ signalling expression score per condition (in MoMFs clusters). Below are shown major $FcR\gamma$ signalling genes; MoMFs clusters 9 and 17 percentages, and double-violin plots of *Fos* gene (n \geq 2), all from scRNA-Seq 10X analysis. **(V)** Representative images of immunofluorescence triple staining for FCER1G/CD11b/Ly6C on liver sections of WT ND, WT CD-HFD and $FcR\gamma^{-/-}$ mice. **(W)** Quantification of triple and double staining (CD11b/Ly6C) in WT ND, WT CD-HFD and $FcR\gamma^{-/-}$ mice (n=4), and quantification of triple staining in WT ND and WT, WT α CD20-treated, μ MT, IgMi, AIDg23s mice under CD-HFD (n \geq 3). **(X)** Representative images of IHC staining for FCGR1, p-HCK on liver sections of WT ND and WT, $JH^{-/-}$, WT α CD20-treated, μ MT, IgMi, AIDg23s mice under CD-HFD. All data are presented as mean \pm SEM. Statistical analyses were performed using unpaired T-test. The scale bar represents 100 μm .

Fig. S6: Germ-free mice develop NASH under CD-HFD, acerbated by B-cells.

(A) Body weight development (n=6). **(B)** Glucose tolerance test assessed on 6-months GF WT ND and GF WT CD-HFD (n=4). **(C)** Quantifications of liver flow cytometric analyses comparing 6-month GF ND, and GF CD-HFD for total CD19⁺ cells and total CD3⁺ cells (n=4). **(D)** Treatment scheme for the B-cell depleted GF WT CD-HFD male mice. **(E)** Serological ALT and cholesterol levels in 4-month (start of the depletion treatment) GF ND and GF CD-HFD male mice (n \geq 6). **(F)** Representative B220 staining of spleen sections of WT control and α CD20-treated CD-HFD mice. **(G)** Summary Table Sindicating clinical data as follows:

serological ALT values, cholesterol, hepatic triglycerides, NAS and phenotypic outcome for germ-free (GF) WT ND and GF CD-HFD. Unpaired T-test statistical analysis for: a) GF CD-HFD vs GF ND; b) α CD20 GF CD-HFD vs GF CD-HFD (n \geq 4). **(H)** Representative H&E staining of liver sections derived from GF WT CD-HFD untreated or treated with α CD20. **(I)** Representative Sudan red staining, and **(J)** quantification (n=5). **(K)** Flow cytometry quantification of hepatic total CD8⁺ cells, total CD8⁺CD62L⁺ and CD8⁺CD62L⁻ cells, total and CD8⁺perforin^{high} and CD8⁺TNF⁺ cells, comparing GF CD-HFD and GF CD-HFD α CD20-treated groups (n=4). Displayed below, absolute quantification of liver flow cytometric analyses of CD19⁺ cells or CD3⁺ cells; normalized to Mode histogram of CD20⁺ cells of CD45⁺ cells in pancreatic WT control and α CD20-treated CD-HFD groups; and percentages of CD45⁺ cells of CD20⁺CD19⁺ cells comparing GF CD-HFD and α CD20 GF CD-HFD (n=4). **(L)** Representative IHC images of liver sections and quantifications per mm² for B220, CD3, F4/80 and MHCII staining of GF ND and GF α CD20-treated CD-HFD mice (n=5). All data are presented as mean \pm SEM. Statistical analyses were performed using unpaired T-test or ANOVA. The scale bar represents 100 μ m.

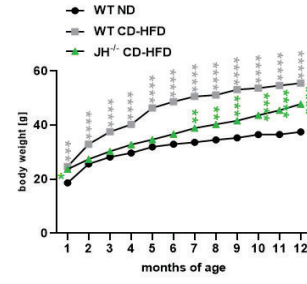
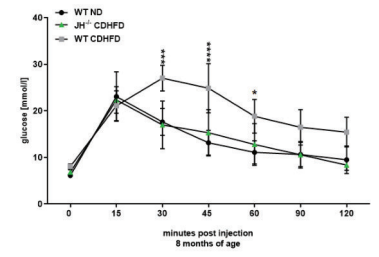
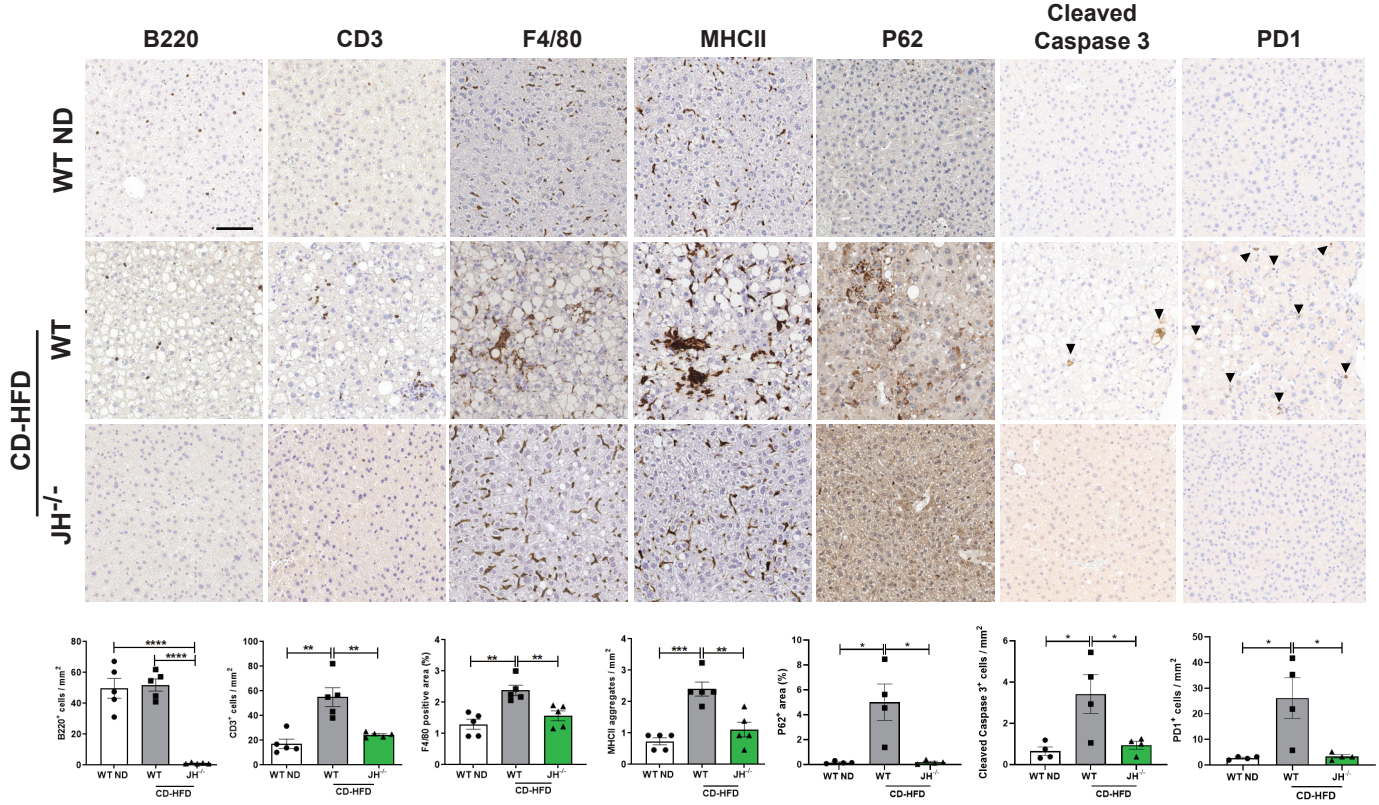
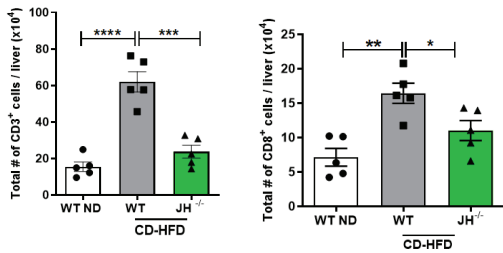
Fig. S7: Fibrosis does not associate with increased Kupffer cells but rather with SAMacs, which display upregulated FcR γ signalling

(A) Representative IHC images showing jejuna p-SYK positive immune cells (per mm²) (n \geq 5). **(B)** Serological measurement of IgA, IgG and IgM levels in NAFLD patients divided in two subgroups (F0-F2 and F3-F4) based on fibrosis score (Brunt/Kleiner scoring) (n \geq 14 each group, total n=33). **(C)** Correlation of IgA levels (g/L) with NAS in NAFLD patients (n=639). **(D)** Gene expression correlation of *FCER1G* against *CCR2*, or against *S100A4*, in the overall NAFLD patient cohort (n=206). Correlations are performed using normalized reads, corrected for sex and batch effect. **(E)** Serological ALT measurement of obese patients (body mass index, BMI \geq 30) treated with rituximab for rheumatoid arthritis (n=15), and on the right are

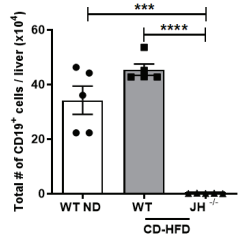
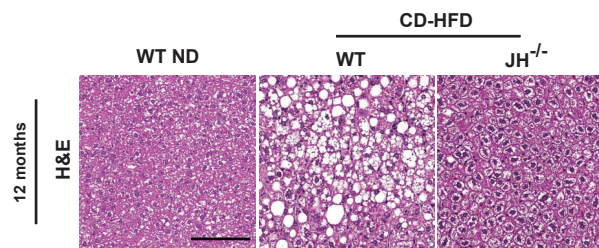
displayed only the responders (n=11 out of 15). **(F)** Correlation plot of IgA serological levels with portal tract or parenchymal CD8⁺ cells, or **(G)** correlation of IgA with portal tract or parenchymal PD1⁺ cells (n=54). **(H)** IHC representative images of FCER1G, CCR2 and S100A4 in NAFLD patients with absent/very low fibrosis (F0/F1) and high fibrosis (F3) at low magnification. **(I)** Representative IF images for profibrogenic macrophages with FCER1G/S100A4/DAPI markers of liver sections from patients with NAFL, NASH-F2, and NASH-F4. **(J)** Representative IF for phospho-SYK/CD20/CD8 on jejunum sections of NAFL and NASH patients. **(K)** Clustermap of 496 common genes between the human and mouse scRNA-Seq datasets, showing ranked mean expression per liver CD45⁺ cell group (SAMacs, Not SAMacs, MoMFs and Not MoMFs). **(L)** Heatmap showing gene expression values (log values) of significantly different FcR γ signalling-related genes in healthy and cirrhotic livers from scRNA-Seq analysis (n \geq 5). All data are presented as mean \pm SEM. Statistical analyses were performed using unpaired T-test. The scale bar for IHC represents 100 μ m, and for immunofluorescence 50 μ m.

A

Group	Statistics	Serum ALT (U/L)	Serum Cholesterol (mg/dL)	Hepatic triglycerides ($\mu\text{g}/\text{mg}$ tissue)	NAS	Outcome
WT ND 6M	Mean value SEM N	34.22 ± 3.378 9	101.6 ± 7.195 8	26.46 ± 4.122 5	0.25 ± 0.164 8	healthy liver, normal body weight
WT CD-HFD 6M	Mean value SEM N P-value ^a	178.9 ± 17.394 9 <0.0001	271.6 ± 7.187 10 <0.0001	121.8 ± 21.63 5 0.0025	5.125 ± 0.350 8 <0.0001	NASH, obesity
JH ^{-/-} CD-HFD 6M	Mean value SEM N P-value ^b P-value ^c	42.33 ± 5.183 9 <0.0001 0.2083	121.5 ± 3.033 10 <0.0001 0.0141	45.16 ± 8.635 5 0.011 0.0865	1 ± 0.327 8 <0.0001 0.0596	healthy liver, \uparrow body weight

B**C****D****E****G**

Group	Statistics	Serum ALT (U/L)	Serum Cholesterol (mg/dL)	Hepatic triglycerides ($\mu\text{g}/\text{mg}$ tissue)	NAS	Outcome
WT ND 12M	Mean value SEM N	45 ± 2.366 10	135.2 ± 5.802 9	59.8 ± 2.864 5	0.5 ± 0.288 4	healthy liver, normal body weight
WT CD-HFD 12M	Mean value SEM N P-value ^a	183.5 ± 17.869 10 <0.0001	254.7 ± 12.776 10 <0.0001	181.4 ± 20.30 5 0.0003	6.5 ± 0.288 4 <0.0001	NASH, obesity
JH ^{-/-} CD-HFD 12M	Mean value SEM N P-value ^b P-value ^c	44.71 ± 4.258 10 <0.0001 0.9532	186.7 ± 20.745 10 0.012 0.036	55.68 ± 9.990 5 0.0005 0.7018	2.5 ± 0.645 4 0.0013 0.03	healthy liver, obesity

F**H**

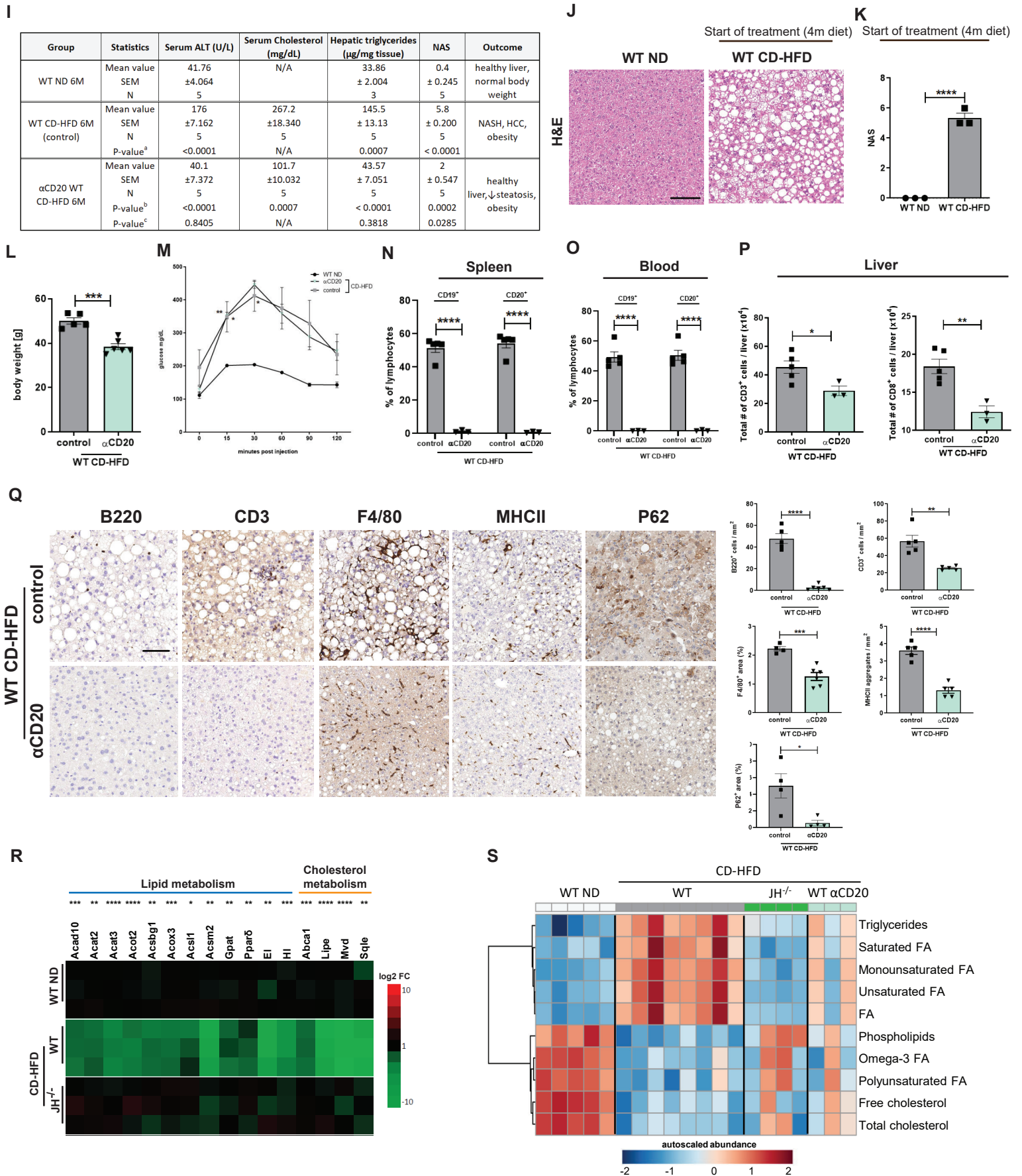


Fig. S1

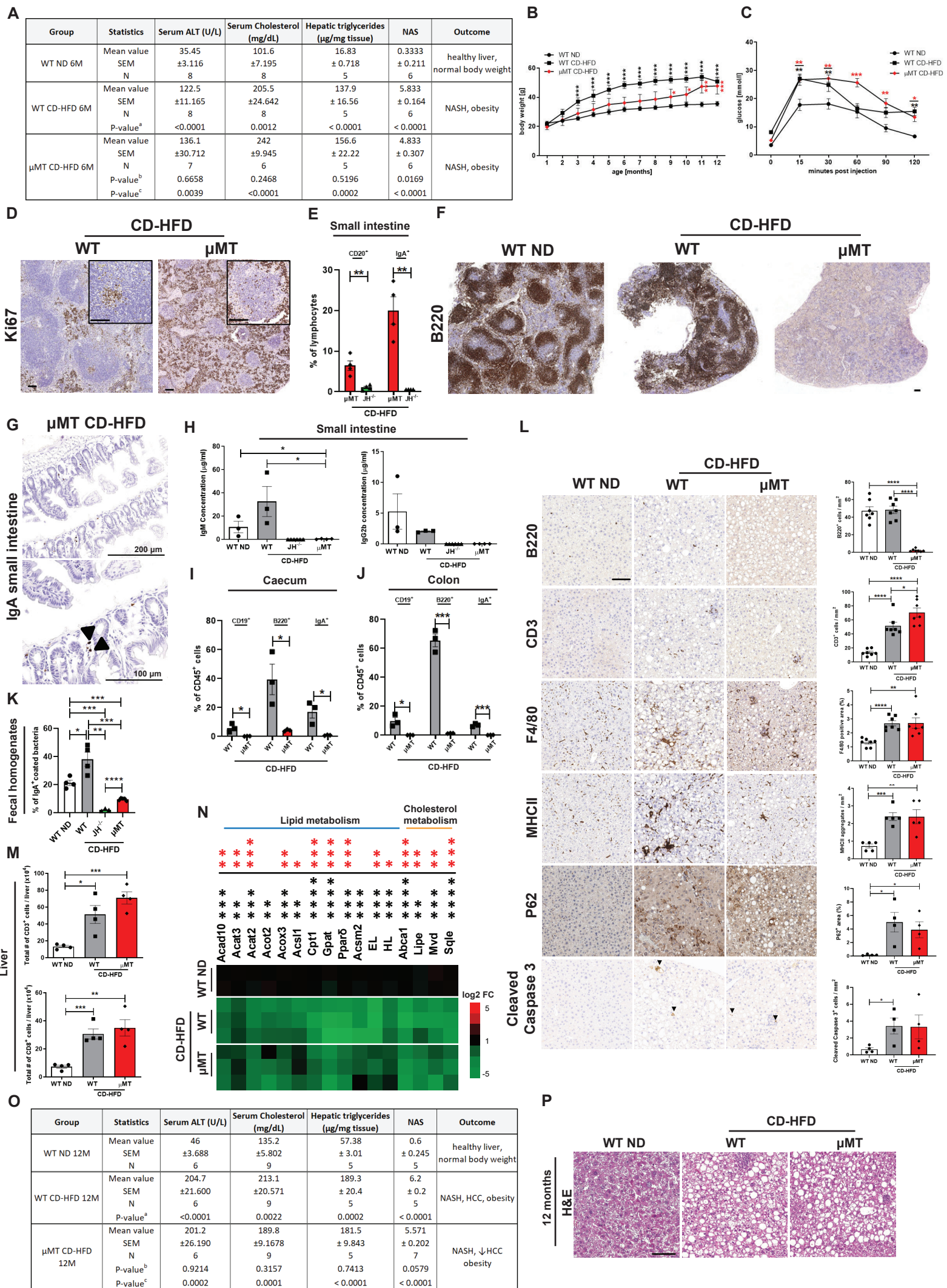
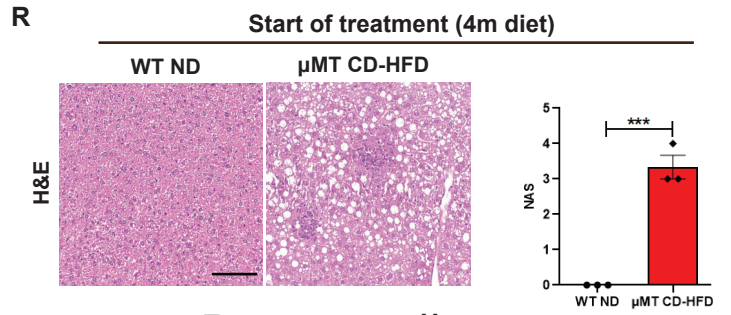
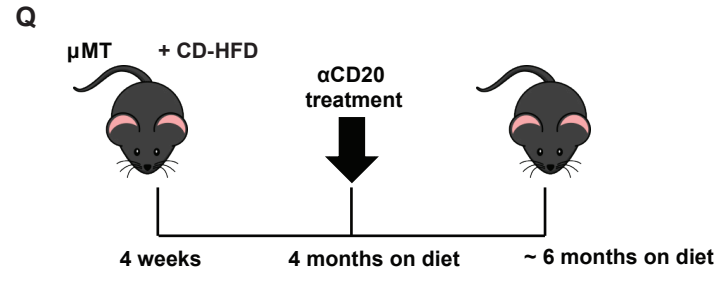


Fig. S2



S

Group	Statistics	Serum ALT (U/L)	Serum Cholesterol (mg/dL)	Hepatic triglycerides (μ g/mg tissue)	NAS	Outcome
WT ND 6M	Mean value SEM N	37.3 ± 2.557 4	N/A	20.67 ± 2.693 4	0.75 ± 0.25 4	healthy liver, normal body weight
μ MT CD-HFD 6M (control)	Mean value SEM N P-value ^b	158.9 ± 14.178 4 0.0002	201.7 ± 2.333 4 N/A	175.6 ± 14.84 4 < 0.0001	5.25 ± 0.25 4	NASH, obesity
α CD20 μ MT CD-HFD 6M	Mean value SEM N P-value ^b P-value ^c	44.45 ± 1.613 4 0.0002 0.0559	189 ± 1.915 4 0.0031 N/A	43.3 ± 16.64 4 0.001 0.2279	1.75 ± 0.25 4 < 0.0001 0.03	healthy liver, obesity

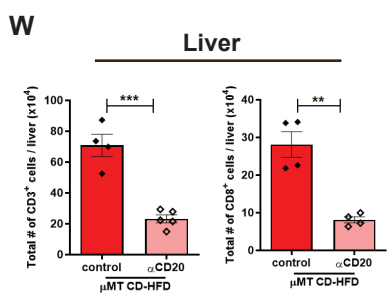
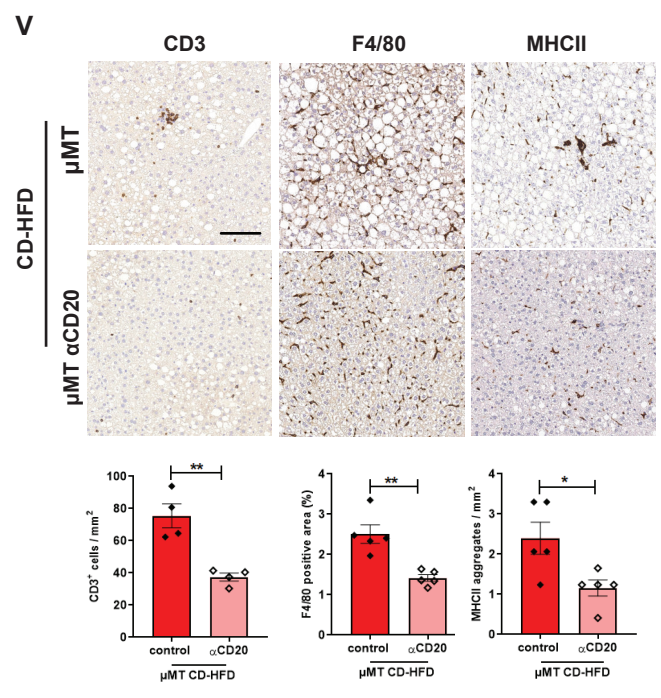
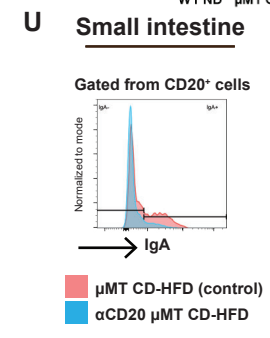
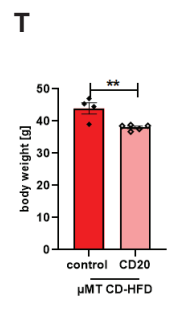


Fig. S2

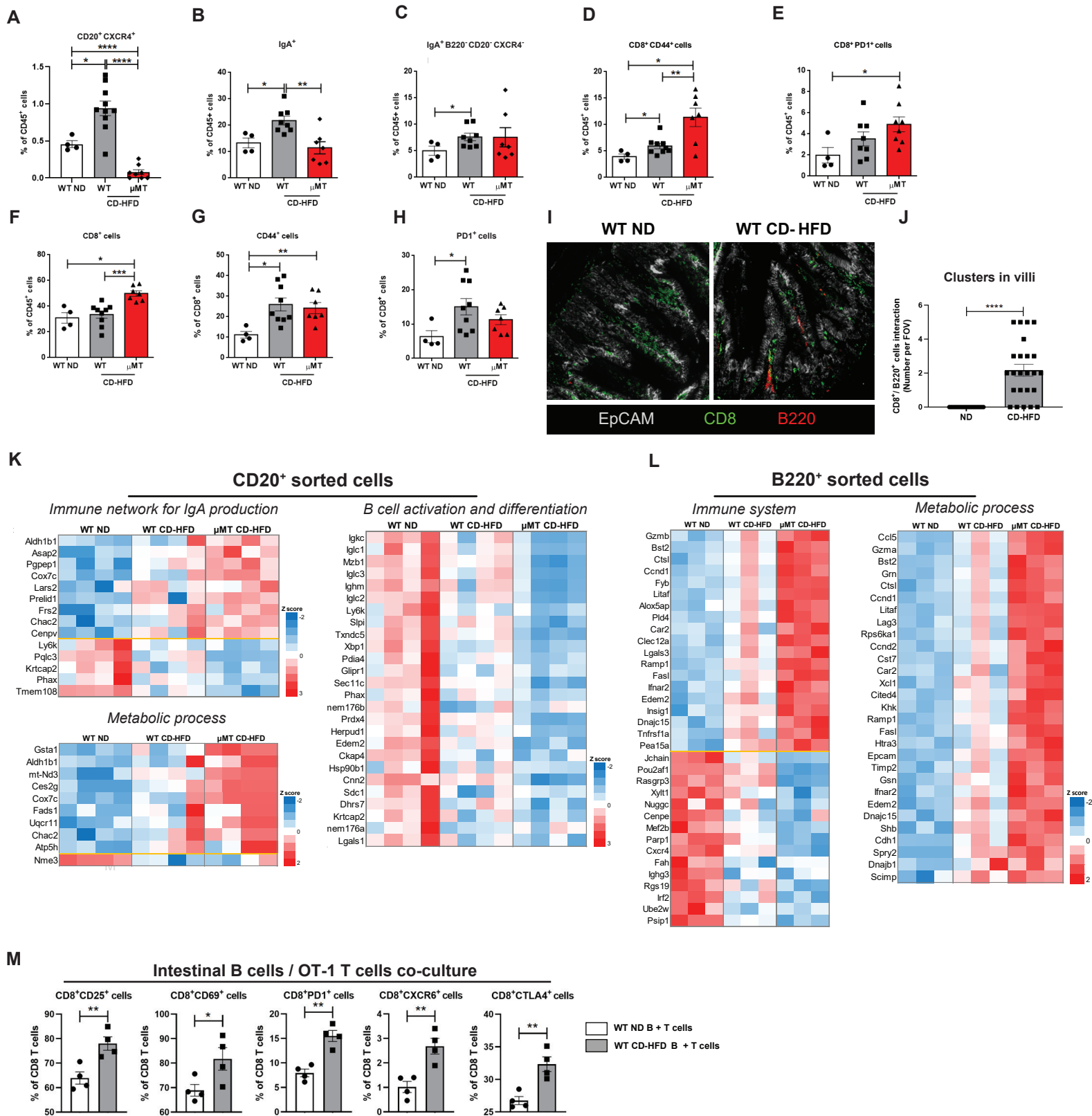


Fig. S3

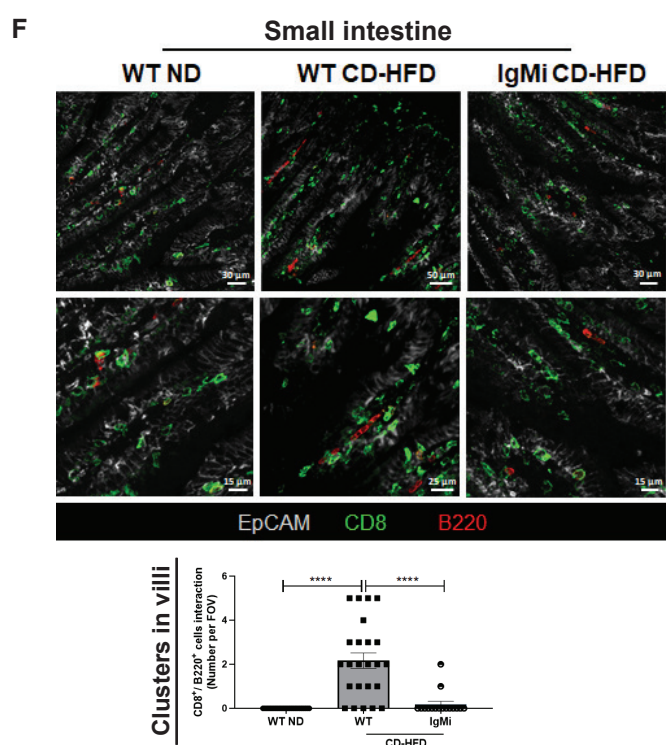
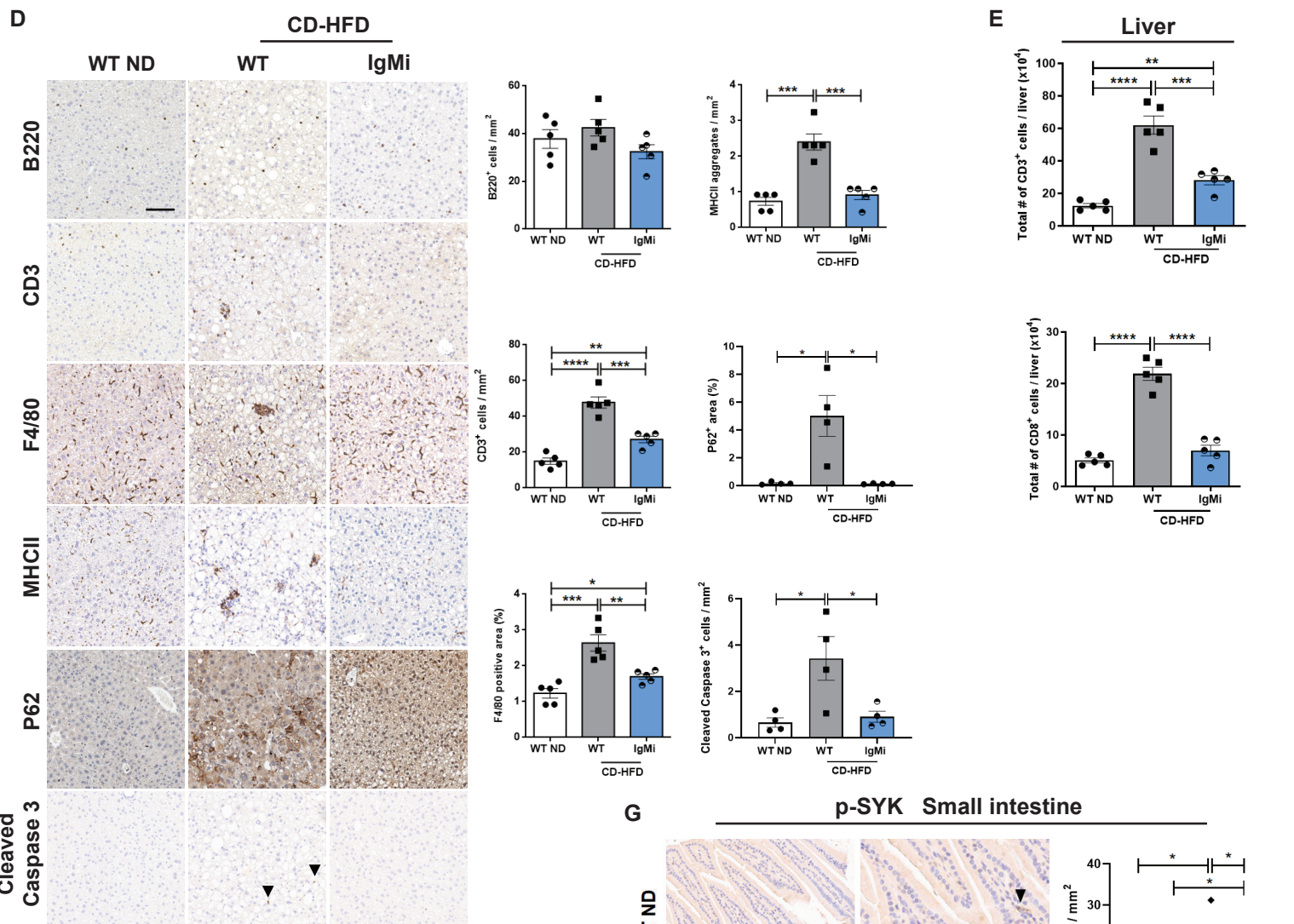
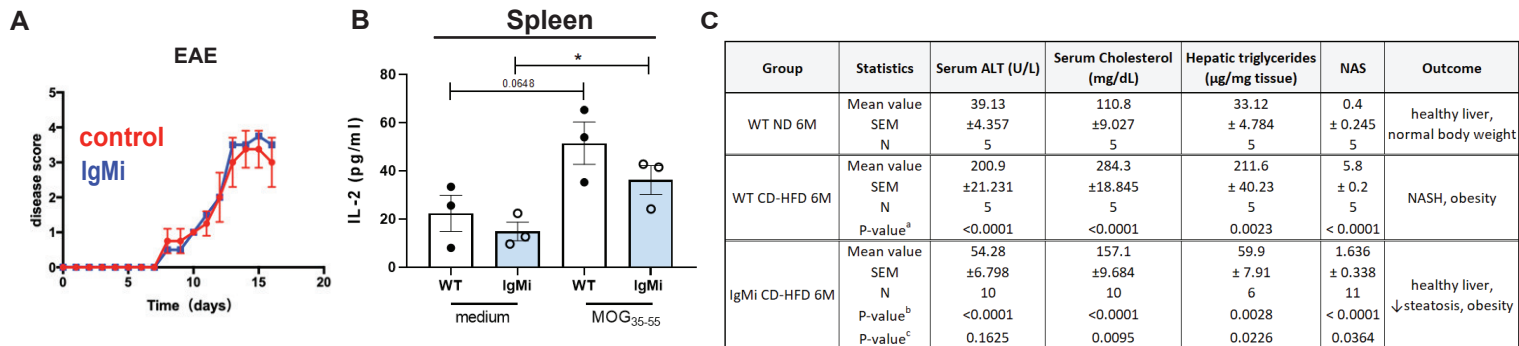


Fig. S4

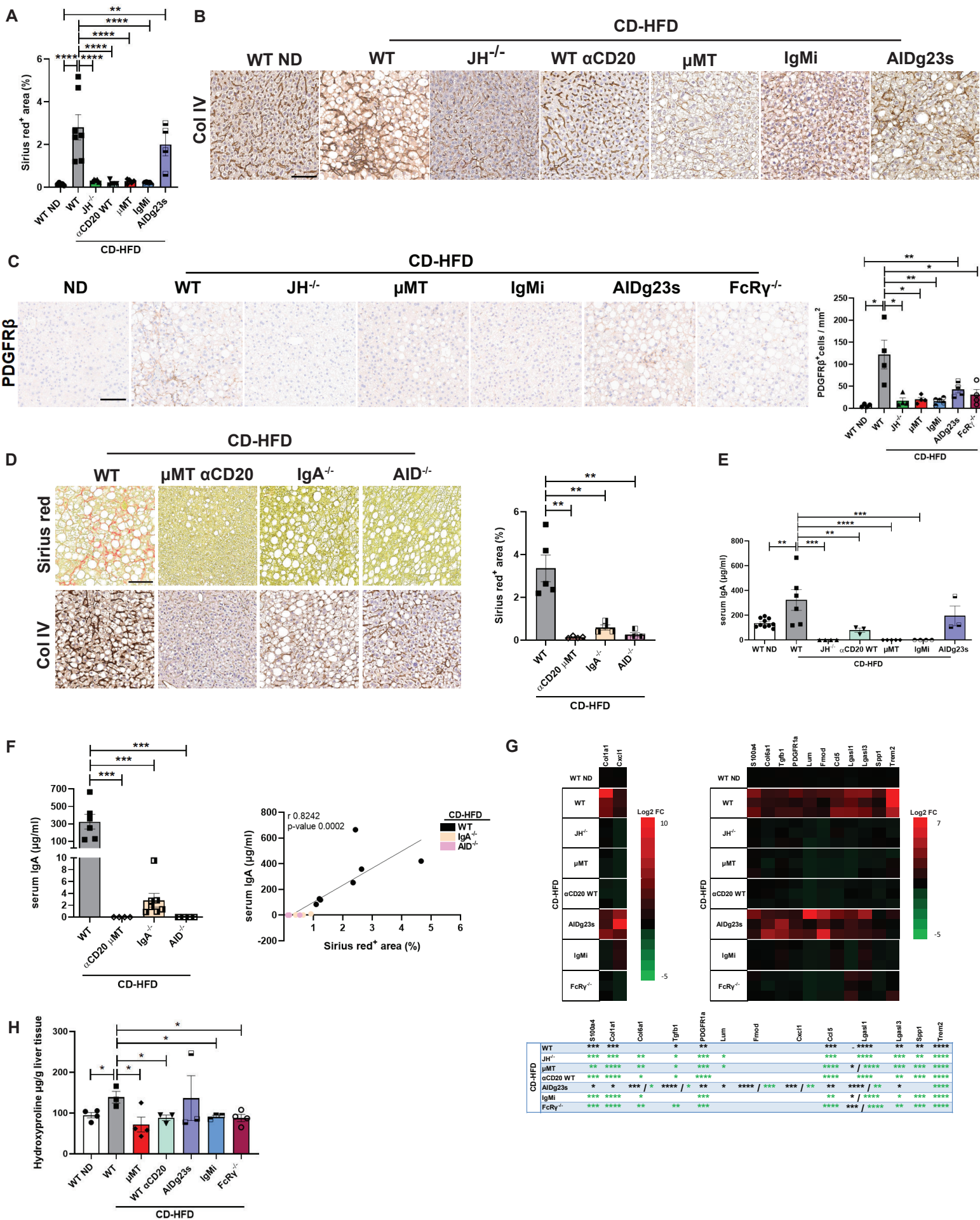


Fig. S5

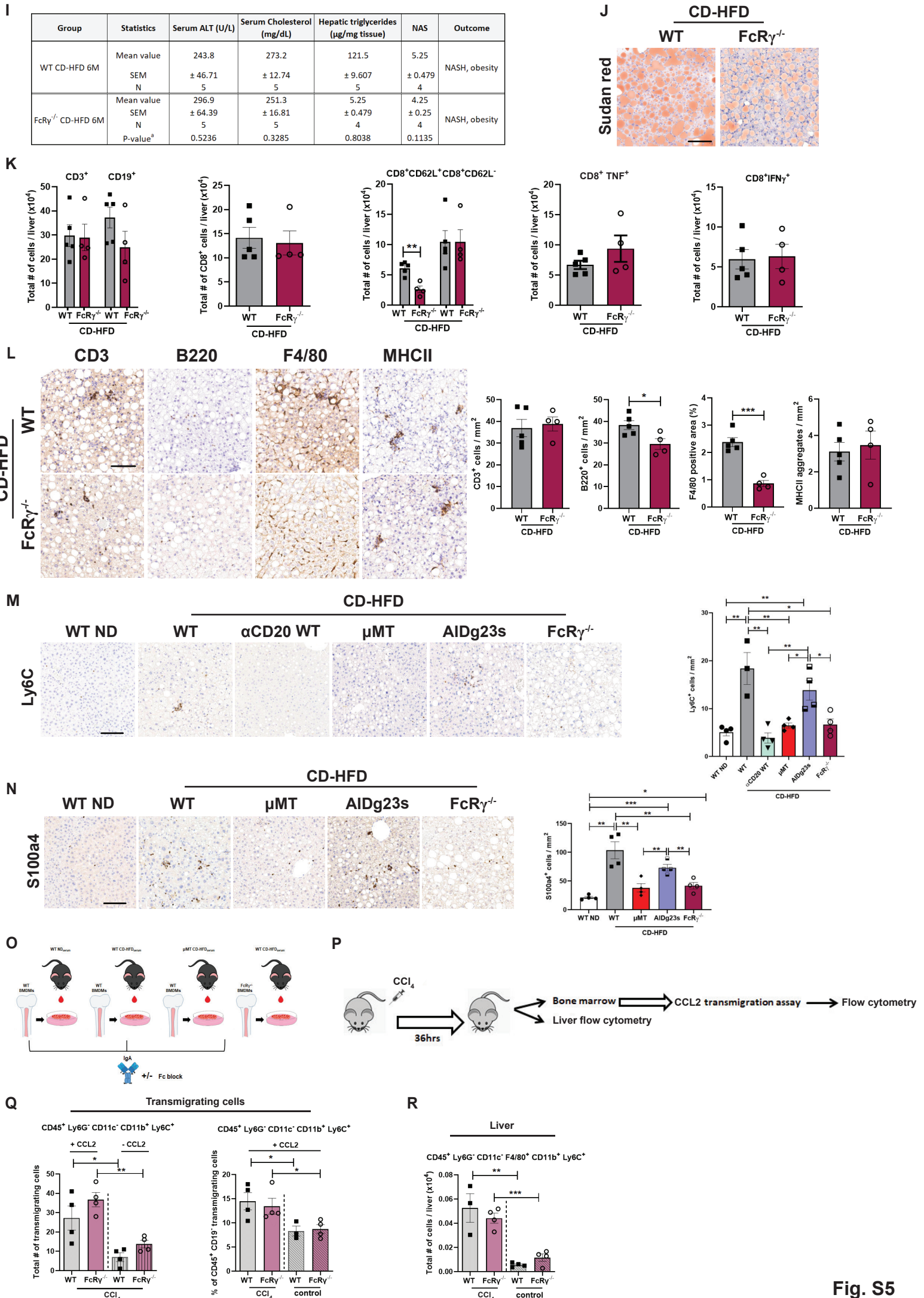


Fig. S5

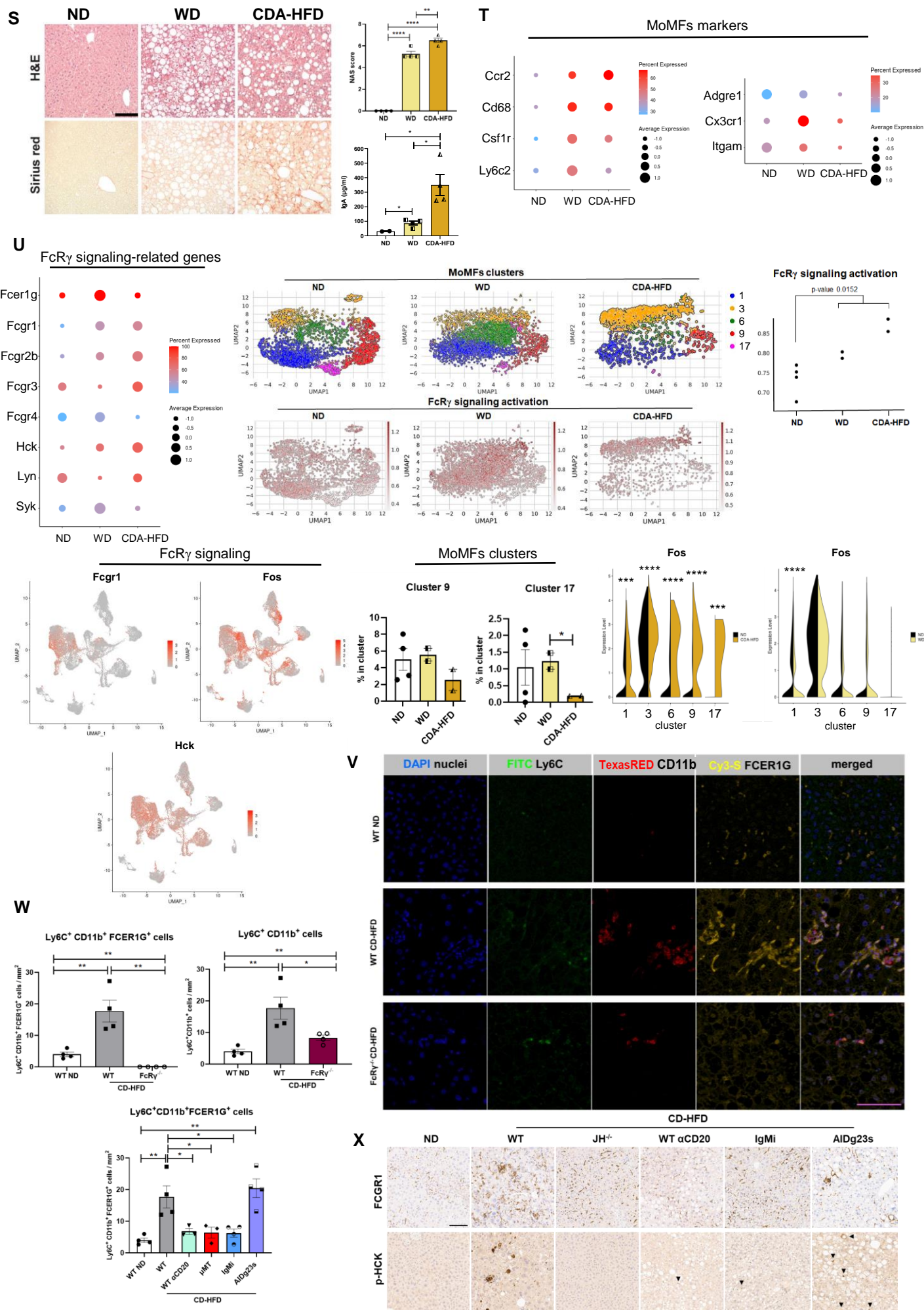


Fig. S5

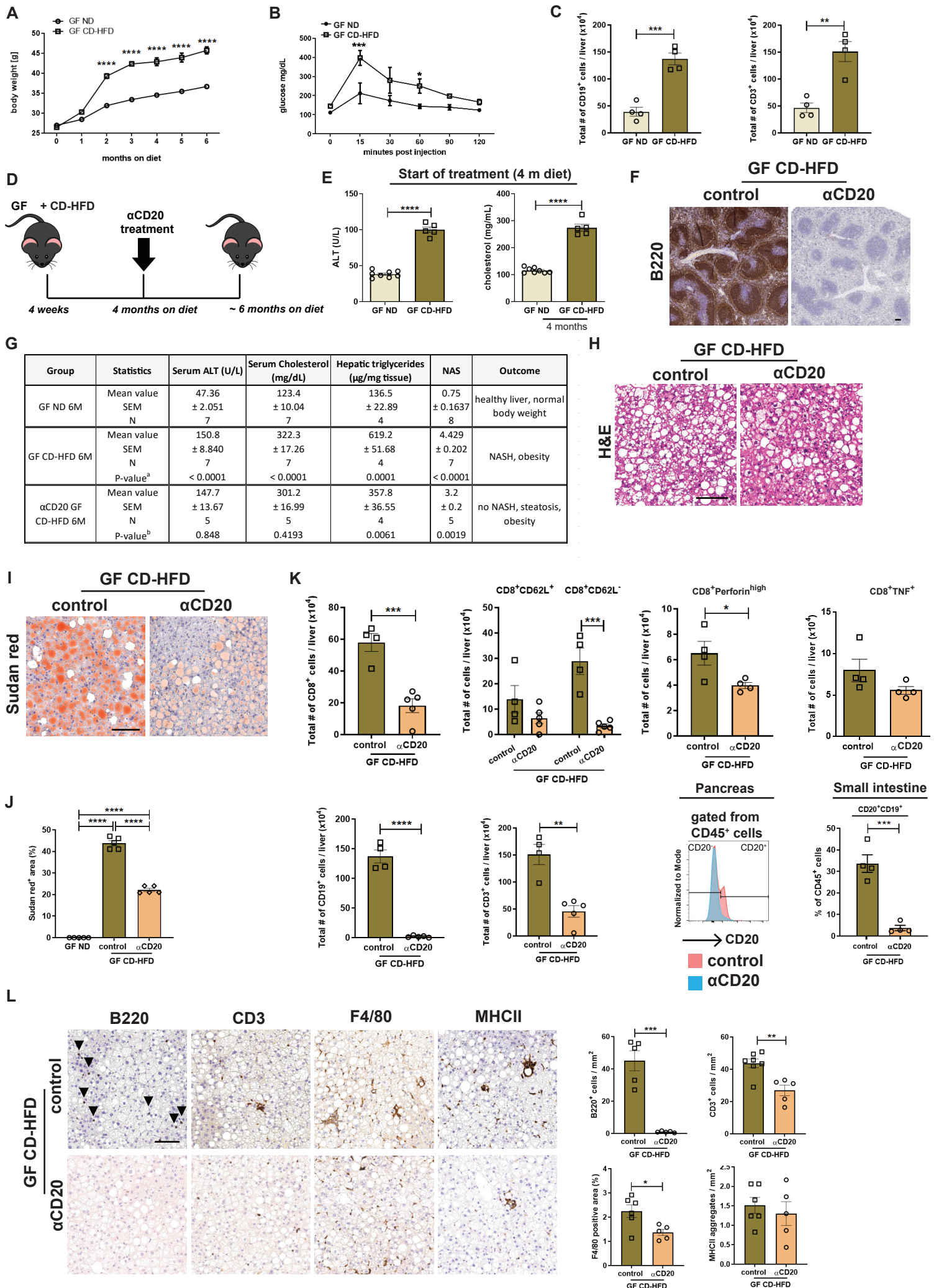


Fig. S6

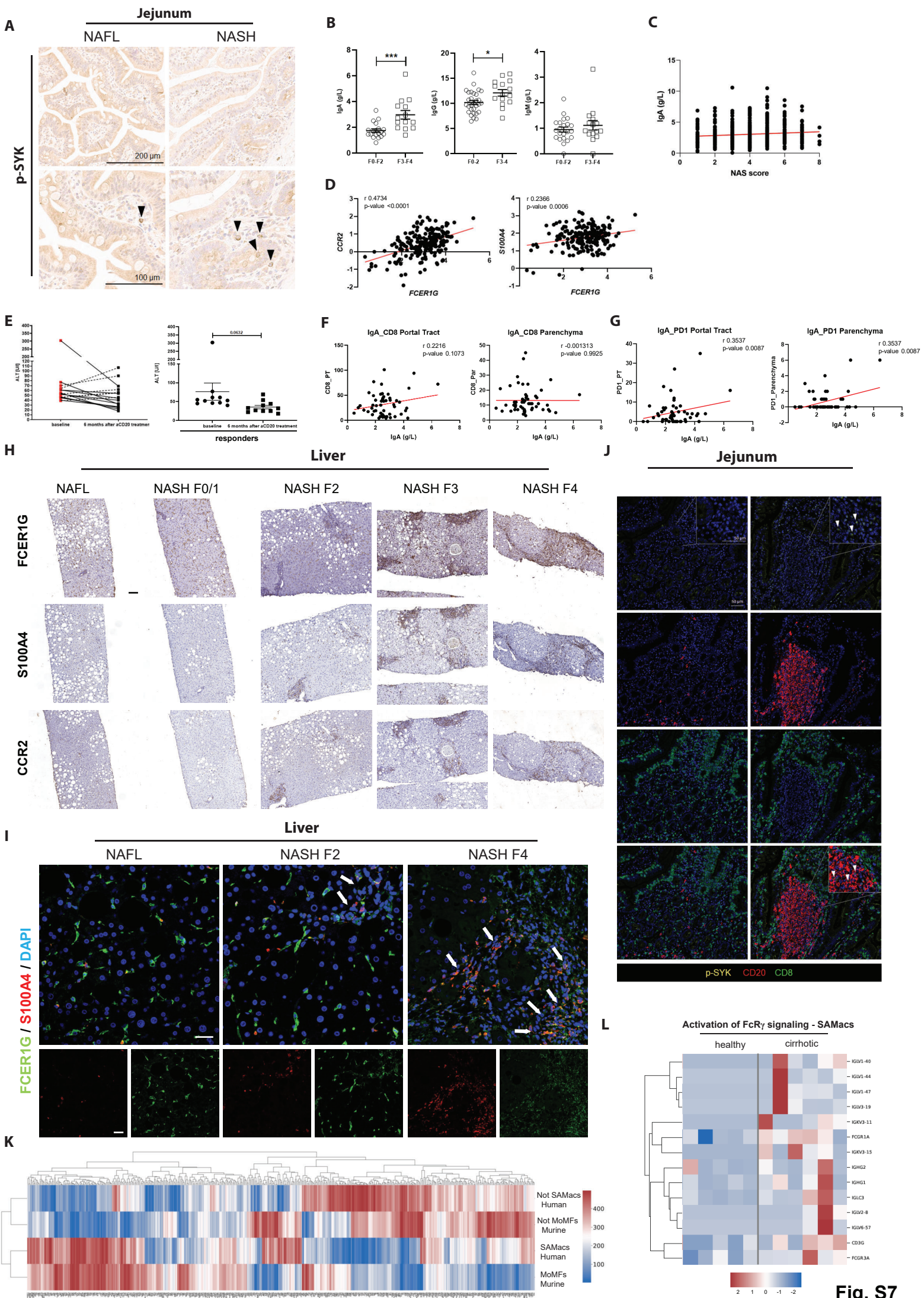


Fig. S7